ORGANOMETALLICS

pubs.acs.org/Organometallics Article

Transition Metal Nitrosyls: Statistics, Charge Estimates via CDVR, and Studies of Tetradentate Chelate Diamides (pddi)M and (pddi)MNO (M = Cr, Fe, and Co)

Alexander A. D'Arpino, Thomas R. Cundari, Peter T. Wolczanski,* and Samantha N. MacMillan

Cite This: *Organometallics* 2023, 42, 2747−2761 Read Online

ACCESS | Metrics & More | Article Recommendations | Supporting Information

ABSTRACT: Correlations of ν(NO) with d(NO), ∠MNO, and charge from roughly 560 first row transition metal complexes are graphically depicted. An equation of charge (c_{NO} = {ν(NO) − 1960}/450 cm^{-1}) was phenomenologically derived within the parameters set by CDVR (charge distribution via reporters) and used to show that nitrosyl should realistically not be interpreted as bound "NO^{+}". The tetradentate chelate [Me_2C{CH═N(1,2-C_6H_4)NH(2,6-$^{i}Pr_2C_6H_3$)$_2$}]^{n} ((pddi)^{n}) was shown to produce (pddi)M (**2**-M; M = Cr, Fe, Co) as precursors to mononitrosyls, (pddi)MNO (**2**-MNO). Significant electronic complexity was observed in 2-M and **2**-MNO (M = Cr and Fe), and **2**-Co was unstable, degrading to {[κ^3-N,N,N-1,2-ArNC_6H_4N═$CHCMe_2$NO]Co}$_2$ (**3**; Ar = 2,6-$^{i}Pr_2C_6H_3$). Structural features of **3** conform to formally S = 1/2 Co(II) centers antiferromagnetically coupled to alkylnitroso radical anions, that is, LS [(LX^{-})$Co^{2+(\uparrow)}RNO^{(-\downarrow)}$][($LX^{-}$)$Co^{2+(\downarrow)}RNO^{(-\uparrow)}$], whose charge elements are consistent with the tenets of CDVR.

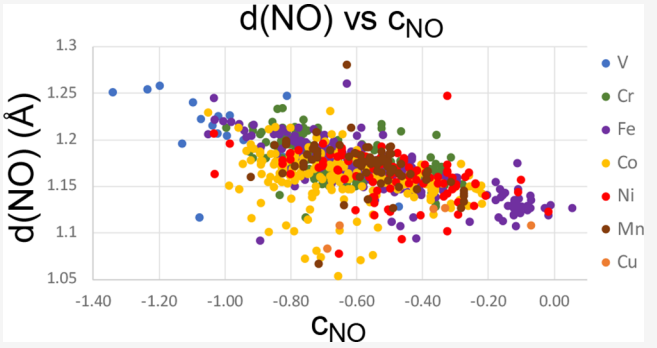

INTRODUCTION

Assessing charge in inorganic and organometallic systems is subject to the methodology utilized in experiment and/or calculation, and reality to the beholder often colloquially relies on "where the dotted lines" have been drawn.[1−9] In addition, the reliance on valence bond theory (VBT) in communicating transition metal (TM) structures through line drawings can lead to misinterpretation of metal−ligand interactions, including charges. At the core of the problem is the need to include and weight all relevant VB structures. Other issues include the absence of—or assumption of—formal charges or when formal charges belie reality, particularly in metal−ligand π-bonding.

A crucial example is NO ligation to transition metals, where traditional electron-counting methods implicate (NO)$^{+}$ when ∠M−N−O is linear (180−165°) and (NO)$^{-}$ when it is bent (140−115°).[10,11] The possibility of neutral NO (160−145°) ligation and its radical character contribute to the difficulty of assessing bonding. Nitrosyls have historically been assessed mainly via IR spectroscopy, where bonding modes (linear: 1960−1600 cm^{-1}; bent: 1750−1600 cm^{-1}; μ_2-, μ_3-bridging: 1650−1350 cm^{-1}) manifest a significant overlap, as correlated with X-ray diffraction.[12−17] The ambiguities presented by NO and frustration in specifying its bonding mode(s) have led to the fairly widespread adoption of Enemark-Feltham notation,[17] in which the sum of d-electrons and NO π*-electrons encompasses several possible configurations, bypassing assignment of a specific metal oxidation state. High energy spectroscopies have been applied more recently and help to provide an additional approach to discern binding modes.[18−20]

The application of VBT is largely the culprit in the often misinterpretation of nitrosyls. In Figure 1, the array of VB structures shown as decreasing NO and increasing NM character exemplifies the difficulties in assigning physical structures to spectroscopic and metric properties. Corresponding assessments of formal oxidation states contribute to the confusion and can obscure the actual important bonding features. For example, consider the VB structures that contribute to "NO^{+}" binding to L_nM, which seems to necessitate a formal (−) charge on the metal. If π-backbonding occurs, and double bonds are used to depict the decrease in NO bond order, application of formal oxidation states (FOSs) akin to an imide renders the nitrosyl an anion and removes the problems affiliated with "NO^{+}" binding.

Neutral NO binding can be portrayed in similar fashion, and again application of the metal FOS paradigm shows it as an anion, as is the case where binding of NO^{-} is considered. For anionic NO binding, it is not necessary for NO^{-} to be bent, as

Received: April 25, 2023
Published: September 13, 2023

https://doi.org/10.1021/acs.organomet.3c00197
Organometallics 2023, 42, 2747−2761

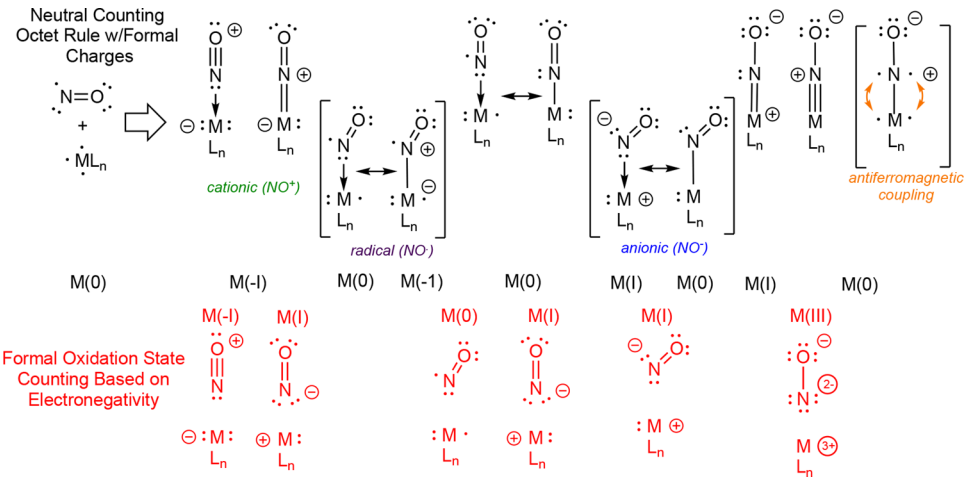

Figure 1. Valence bond (VB) representations of d^n ($n \geq 3$) binding nitric oxide. The octet rule for N and O is strictly obeyed (aside from the neutral radical), including formal charges (a line denotes a shared pair of electrons). Decreasing NO and increasing MN bond order shown left-to-right. Only three d-electrons are needed to assess all reasonable VB structures of MNO; hence, the depictions are {MNO}^{4} in Enemark-Feltham notation. In red, transition metal formal oxidation states are invoked to provide the other extreme.

the disposition of the π-electrons is crucial to linearity. At the limit in the VB line-up, the rendering of double or triple bond character between L_nM and N is indicative of a strong covalent interaction. In FOS parlance, the metal is +3 and the nitrosyl is a trianion. Adhering to the FOS model provides alternatives to "NO$^+$" and shows that NO can ascribe a neutral or anion charge in all binding modes, consistent with spectroscopic properties.

Pauling electronegativities (i.e., N, X = 3.0; O, X = 3.5; TM, X = 1.3−2.5) also contradict the notion that bound $(NO)^+$ is a viable description, as do its corresponding stretching frequencies. Gas phase values of $(NO)^+$, NO, and $(NO)^-$ taken from NIST are 2376, 1904, and 1363 cm^{-1},[21,22] respectively, whereas complexed NO has average frequencies between 1960 and 1450 cm^{-1}, with many of the high energy stretches assigned to {[Fe]NO}^{6} species, where [Fe] is $(CN)_5Fe^{2-}$ with a variety of cations. Bound NO, being attached to a Lewis acid in the simplest sense, is not the same as gas phase NO, and clearly $(NO)^+$ is an unrealistic limiting portrayal even though it may be a convenient e$^-$-counting model. Researchers in nitrosyls have understood this conundrum[10−17] but often stick with convention, presumably since the lexicon of organometallic chemistry and its counting schemes are convenient.

Some recent work has challenged convention in interesting ways.[23−26] Wieghart and DeBeer et al.[23] have persuasively argued that linear MNO bonding can be consistent with NO$^-$. Calculations and experiments on Tp*MNO (M = Co, Ni; Tp* = hydro-*tris*(3,5-Me2-pyrazolyl)borate) depict the cobalt species, whose ν(NO) = 1732 cm^{-1}, as $(NO)^-$ (S = 1) is antiferromagnetically (AF) coupled to unpaired spins on an S = 3/2 Co center. Likewise, diamagnetic Tp*NiNO, with ν(NO) = 1786 cm^{-1}, corresponds to an S = 1 Ni center AF-coupled to $(NO)^-$.

V2C XES measurements by Lu et al.[18] provide experimental partial charges on linear nitrosyls bound to $[(PhS)_3FeNO]^-$ and $[X_2Fe(NO)_2]^-$ (X = PhS and PhO) of −0.58(18), −0.77(18), and −0.95(18), respectively. These studies, coupled with the range of NO stretching frequencies evident in TM complexes, support the premise that charge, or electron density, is always distributed from the metal to the $(NO)^x$ ligand. Questions remain concerning the relative degree of π-backbonding, that is, a phenomenological value for x and whether ready, less complicated assessments can be made.

Pertinent to the discrepancies involving NO are the corresponding metal oxidation states, which are equally problematic. Preceding the Wieghart and DeBeer work,[23] Parkin,[27] using the covalent bond classification (CBC) method,[28,29] provided a cogent discussion of Tp*NiNO, addressing the covalency of the M−N interaction via a molecular orbital rationale. In the CBC method, three d-electrons are required in MNO bonding (i.e., $(NO)^{3-}$) resulting in a d-count that implicates Ni(IV). Unjust criticism of Parkin's argument focused on this extreme FOS representation,[23] when the focus of this work clearly expressed the covalency of the NiN interaction via pertinent molecular orbitals. The effective charge state of Ni is between the Ni(0) (d^{10}) and Ni(IV) (d^6) formal oxidation states, in line with an early assessment of nitrosyl covalency by Gray, who observed that NO and nitride bonding were quite similar based on spectroscopy, computation, and d(MN).[30−32]

Figure 2 illustrates a truncated MO diagram of a metal nitrosyl interaction, providing an alternative to the VBT descriptions in

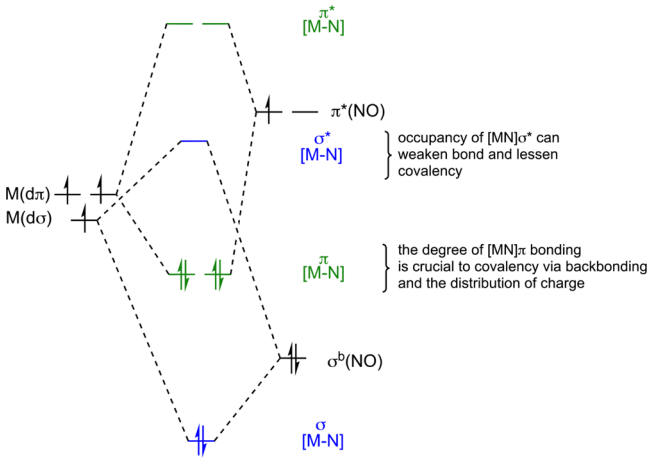

Figure 2. Truncated generic MO description of nitrosyl σ- and π-interactions; various coordination geometries may produce complications due to symmetry and orbital mixing. For a practical discussion of MO treatment, see ref 24.

https://doi.org/10.1021/acs.organomet.3c00197
Organometallics 2023, 42, 2747−2761

Figure 1, with the two summarizing the nitrosyl problem. How do you assess the distribution of fractional charge in NO, when one method (VBT) uses integral charges, rendering the purveyor to weight various depictions, and the other (MO) requires you to partition electron density? In attempting to provide relative numerical charges that are easily grasped within a simple framework, charge distribution via reporters (CDVR)[33] was explored as a means of correlating ν(NO) and the value of x in $(NO)^x$. CDVR has proven to be surprisingly informative in assessing late TM bonding,[34−39] especially carbonyls, and plenty of nitrosyl complexes provide ample statistics to interpret.

Seeking representative mono-nitrosyl complexes, new tetradentate chelates were prepared as plausible metric reporters of NO binding that are readily interpretable by CDVR, instead of requiring calculation.[23,24] What ensued was a morass of electronic complications, unusual spectroscopic observations, and an NO triggered ligand degradation that typify the consequences of nitrosyl chemistry.

RESULTS AND DISCUSSION

Equations of Charge. Equations of relative charge were sought based on CDVR, where charges of metals and ligands are assessed relative to a reference, that is, Fe(+2.0);[33] the method is purported to be a benchtop way of rationalizing charge distribution in a molecule quickly to give insights without the need of computation. The equation of charge for CO is shown in eq 1, where c_{CO} is the resultant charge and ν(CO) is the average stretching frequency. Assessment of different ligands can be obtained from $[M(CO)_xL_y]^p$ complexes[11−17,40−47] using eq 2, where p is the complex ion charge, c_M

$$c_{CO} = (\nu(CO) - 2207\ cm^{-1})/475 \quad (1)$$

$$p = c_M + x_{CO}c_{CO} + y_L c_L + z_{L'}c_{L'} + ... \quad (2)$$

is the CDVR metal charge (for this work: Cr(+2.6), Fe(+2.0), Co(+1.6)), x_{CO} is the number of CO ligands, c_{CO} is the corresponding charge, and y_L is the number of L, the ligand of interest. In the simplest case of CO and L, solving for c_L affords the average charge of L.

Andrews and Citra[45] have generated 52 $M(NO)_X$ (x = 2−4; 33 independent) species by matrix isolation in Ne(s) and Ar(s), whereas only $Cr(NO)_4$ can be prepared under ambient conditions.[46] In cases of neutral species, $c_{NO} = -c_M/x_{NO}$, there is a correlation between charge, c_{NO} and ν(NO) but the average stretches only vary from 1531 cm^{-1} ($Ti(NO)_2(Ar)$) to 1782 cm^{-1} ($Co(NO)_2(Ar)$). Although the equation of the charge produced ($c_{NO} = (\nu(NO) - 1962)/286$)) appears quite reasonable, dispersion of the data is insufficient (R^2 = 0.49).

Given insufficient confidence in the c_{NO} value from Figure 3a, a correlation between ν(NO) and ν(CO) was sought to provide a means of assessing backbonding in NO vs CO leading to an equation of charge. Using 103 complexes with CO and NO as common ligands, a correlation between the two stretching frequencies (each averaged when necessary) was obtained a shown in Figure 3b. The comparison, while somewhat crude, suggests that NO is effectively quite similar to CO in backbonding capacity. Note that the dispersion of NO values in the statistical study below ranged from 1450−1960 cm^{-1}, essentially the same spread as one can confidently assign to metal carbonyls (1670 cm^{-1} ($M(CO)_5^{3-}$, M = Nb, Ta) to 2250 cm^{-1} ($M(CO)_4^{2+}$, M = Pd, Pt)).

Nitrosyl Complex Metrics and Charge. In establishing the equation of charge for CO, the ν(CO) value for $Fe(CO)_6^{2+}$

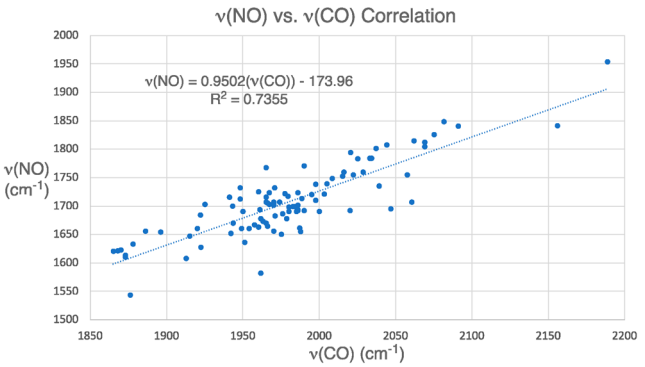

a.

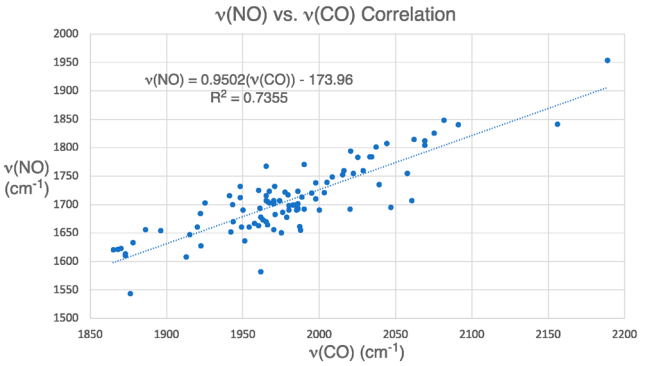

b.

Figure 3. (a) Nitrosyl charge, c_{NO}, from CDVR (eq 2) vs ν(NO) from 52 matrix isolated $M(NO)_X(g)$ (x = 2−4; g = Ne, Ar). (b) Dispersion of ν(NO) values relative to ν(CO) taken from 103 $[ML_x(CO)_y(NO)_z]^p$ complexes.

of ∼2207 cm^{-1} was taken as a limit where c_{CO} = 0.00. Using nitrosyl-containing structures in the Cambridge Crystallographic Database (CCD; the first row TM data set is provided in Supplemental Information), various cations of $[(CN)_5Fe(NO)]^{2-}$ stand out as having ν(NO) in the mid 1900s. A frequency of 1960 cm^{-1} was taken as the limiting value of uncharged NO, where an observed stretch of 1960 would have a c_{NO} = 0.00. The variation of nitrosyl stretching frequencies vs CO in $[ML_x(CO)_y(NO)_z]^p$ complexes in Figure 3b is $\Delta\nu$(NO) ∼ 0.95$\Delta\nu$(CO); hence, the related slope for nitrosyls is

$$c_{NO} = (\nu(NO) - 1960\ cm^{-1})/450 \quad (3)$$

taken to be 1/(0.95(475)), that is, ∼95% of the carbonyl eq 1 value, and a phenomenological equation of charge (relative to c_{Fe} = +2.0; i.e., eq 1) is eq 3. Despite the poor statistics in Figure 3a, it is gratifying to note that a related limiting value of 1960 cm^{-1} was obtained from this attempt at charge evaluation.

Statistics of Randomly Selected Nitrosyls. Using the CCD, various metric parameters of first row transition metal−nitrosyl complexes were compiled to assess the correlations with ν(NO) and with charge (eq 3). The compounds, which were chosen randomly, omitting bridging species, totaled ∼557: V (18), Cr (124), Mn (56), Fe (138), Co (146), Ni (69), and Cu (6). While there was substantial redundancy in terms of similar compounds, the volume of species, as shown via the plots above, seemed to show an appropriate level of dispersion in values.

Figure 4 shows plots of the correlations between ν(NO) (cm^{-1}), d(NO) (Å), and ∠MNO (°), whose various colors are

https://doi.org/10.1021/acs.organomet.3c00197
Organometallics 2023, 42, 2747−2761

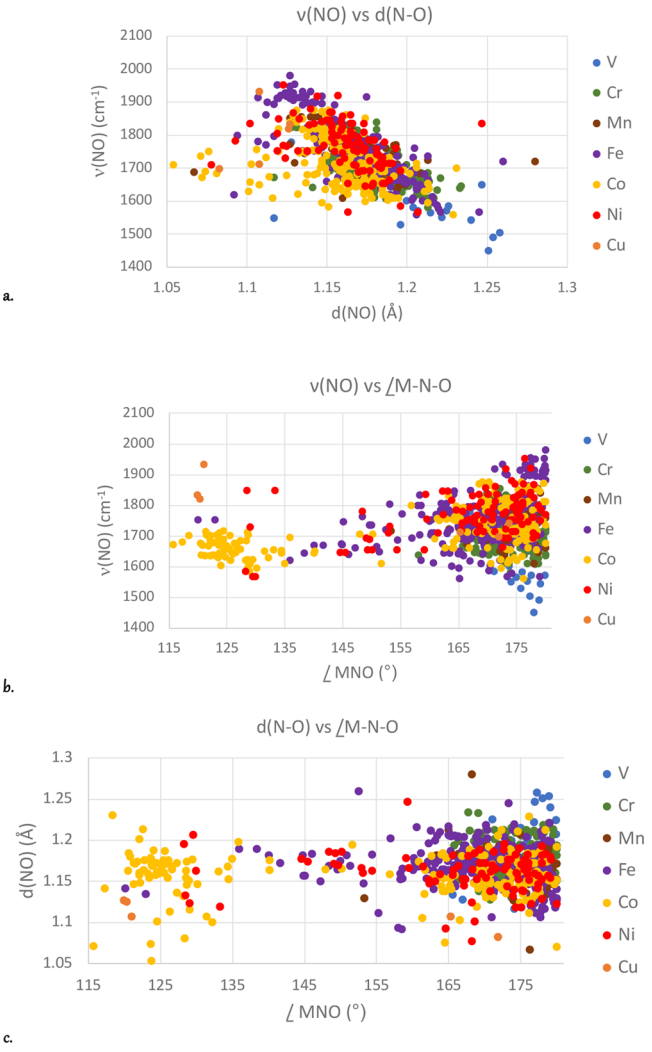

Figure 4. (a) Nitrosyl stretching frequency (ν(NO) in cm^{-1}) vs nitrogen−oxygen distance (d(NO) in Å). (b) Nitrosyl stretching frequency (ν(NO) in cm^{-1}) vs metal−nitrogen−oxygen angle (∠(MNO) in °). (c) Nitrogen−oxygen distance (d(NO) in Å) vs metal−nitrogen−oxygen angle (∠(MNO) in °).

attributed to the different first row transition metals. Figure 4a reveals a general trend for ν(NO) vs d(NO) showing higher stretching frequencies correlating with shorter distances as expected, with a rough slope of ~2.7 × 10^{-4} Å/cm^{-1} (0.27 pm/cm^{-1}; ~3.7 × 10^{3} cm^{-1}/Å or 3.7 cm^{-1}/pm; ν(NO in cm^{-1}) ~ −3720(cm^{-1}/Å)(d(NO) in Å) + 6100 cm^{-1}). Note that also the bulk of the data (>90%) falls to the lower left of a linear trendline for NO^{+} (g), NO (g), and NO^{-} (g) (d(NO in Å) = (8417 cm^{-1} − ν(NO in cm^{-1}))/5462 cm^{-1} Å^{-1}), supporting the contention that bound NO does not have the same charge distribution (analogous to frequency; ν(NO in cm^{-1}) ~ {(−5462 cm^{-1}/Å)(d(NO) in Å) + 8417 cm^{-1}} as free NO. Given that d(NO) is a metric among light atoms, the main trend is reasonable noting standard errors typically run from ~0.02 Å in older crystal structures to ~0.002 Å accorded more modern data collections. It seemed plausible that d(MN) might afford a more accurate distance correlation with ν(NO), but this proved not to be the case (see Supporting Information).

There are a considerable number of outliers, predominantly where M = Co in the 1600−1750 cm^{-1}, where the dependence of ν(NO) on NO distance is minimal. In Figure 4b, the correlation between ν(NO) (cm^{-1}) and ∠MNO (°) is presented and most of the outliers are recognized as "bent" nitrosyls, with angles between 116−137°. What is clear from Figure 4a,b is that ν(NO), here recognized as a reporter of charge, does not ascribe to a particular bonding motif, as a variety of bent, linear, and possibly neutral NO species all have similar frequencies. It can be stated that bent nitrosyls are limited to the 1600−1750 range, aside from Cu compounds, but it must be acknowledged that plenty of linear species exist with these frequencies.

Finally, Figure 4c illustrates the plot of d(NO) (Å) vs ∠MNO (°) that essentially parallels those of Figure 4b as stretching frequency and distance are strongly correlated. Remember that d(NO) does not vary that greatly and that the scatter in the data is impacted by the precision of light atom distance measurements adjacent to heavy atoms, which can sometimes be problematic.

Figure 5 shows a plot of d(NO) (Å) vs $\mathbf{c}_{NO}$ according to eq 3, showing that there is roughly a ~ (−0.12 Å) change in NO

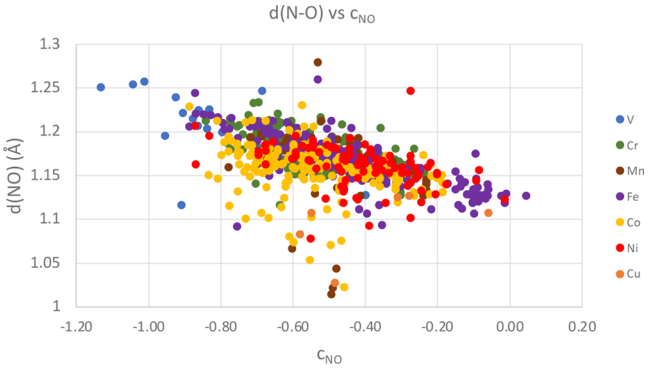

Figure 5. Scatter plot of d(NO) in Å vs $\mathbf{c}_{NO}$ according to eq 3 ($\mathbf{c}_{NO}$ = {ν(NO) − 1960}/450 cm^{-1}).

distance (equivalent to 450 cm^{-1} change in ν(NO)) which results in unit charge. Given that eq 3 generates $\mathbf{c}_{NO}$ for any ν(NO), Figure 5 is related to Figure 4a with $\mathbf{c}_{NO}$ replacing frequency on one axis. The 1600−1700 cm^{-1} NO frequencies attributed to bent NO correlate to roughly −0.75 to −0.45 units of charge, showing that even as a conventional "nitrosyl anion", covalency can attenuate charge in the CDVR model (referenced to $\mathbf{c}_{Fe}$ = +2.0), where similarly charged carbonyls range from 1850 to 1990 in frequency.

Most nitrosyls are within an angular range sufficient to be classified as linear, and their charges range from 0.0 to −1.17. π-Backbonding is expected to be the most significant for early metals, paralleling carbonyl examples, due to better energy match of metal 3d and NO π^*-orbitals (Figure 2), and many low frequency examples are vanadium. It is critical to note that in this model, anionic nitrosyl can still withdraw charge from the metal in π-backbonding, as the charges <−1 attest.

One might legitimately consider CDVR biased in this study due to the choice of 1960 as a likely limit for zero charge. As a fair comparison, Figure 6 illustrates the distribution of charges vs d(NO) derived from an equation of charge calculated from NO^{+} (g), NO (g), and NO^{-} (g): $\mathbf{c}_{NO}$ = {ν(NO) − 1854}/500 cm^{-1}. The pattern is obviously the same as Figure 5 but shifted, and now there are a smattering of nitrosyls that have some net, fractional positive charge. While most of the species are cations, the vast majority of Fe species are variants of [(CN)$_5$Fe(NO)]$^{2-}$ and a few are carboxamides (e.g., (bcb)Fe(NO$_2$)(NO) and macrocycles (e.g., [(OEP)FeNO]$^{+}$). The cobalt species are

https://doi.org/10.1021/acs.organomet.3c00197
Organometallics 2023, 42, 2747−2761

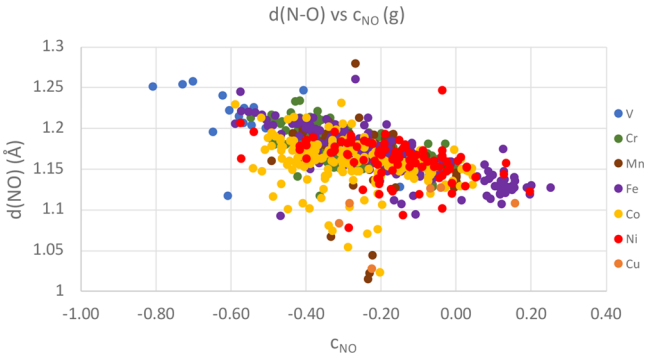

Figure 6. Scatter plot of d(NO) in Å vs c_{NO} according to equation of charge derived from NO^n (n = −1, 0, 1); c_{NO} = { ν(NO) − 1854}/500 cm^{-1}).

$[L_2Co(NO)_2]^+$ and $[L_3Co(NO)]^+$ cations; the nickel compounds are all mononitrosyls $[L_3Ni(NO)]^+$, and the copper species is $[(MeNO_2)_3Cu(NO)]^{2+}$ (see SI for references). Note that this line of charge, biased because the gas phase components are not attached to a Lewis acid, fails to show any charge remotely close to +1.

Tetradentate Chelates. The tetradentate chelate $[\{-CH{=}N(1,2\text{-}C_6H_4)NH(2,6\text{-}{}^iPr_2C_6H_3)_2\}]^n$ ((dadi)^n) has been shown to metrically respond to changes in electron density.[48−51] The redox non-innocence (RNI) is observed via elongation of the imine carbon-nitrogen bonds from 1.299(4) Å to single bond distances (1.381(8) Å) and concomitant shortening of the C−C ligand backbone from 1.432(2) Å to a double bond distance (1.346(5) Å), as shown in Figure 7. Given

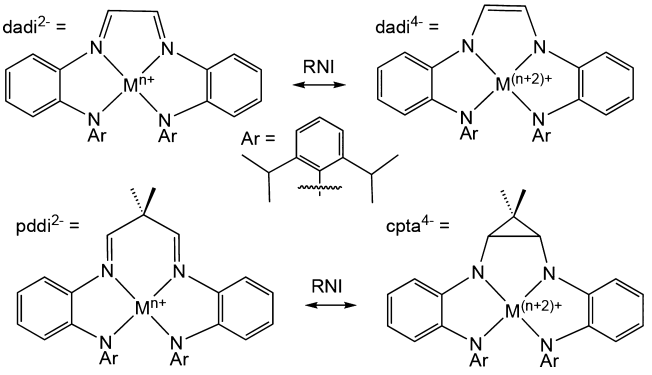

Figure 7. Redox non-innocence (RNI) of dadi^n and the corresponding proposed RNI for pddi^n, featuring potentially reversible C−C bond formation.

the possibility of fractional charge distribution, nitrosyls were thought to be a ligand with competitive electron-withdrawing power, inducing subtle yet detectable changes. A different type of RNI was considered in which a sterically related chelate $[Me_2C\{CH{=}N(1,2\text{-}C_6H_4)NH(2,6\text{-}{}^iPr_2C_6H_3)_2\}]^n$ ((pddi)^n) could reversibly form a cyclopropane C−C bond.[52−55] The d(CC) could conceivably be used to estimate its BDE,[56] leading to some thermodynamic information regarding RNI.

As previously described,[57] Swern oxidation of 2,2-dimethyl-1,3-propanediol to the dialdehyde was conducted, to which two equiv. 1,2-(2,6-$^iPr_2C_6H_3NH$),$NH_2C_6H_4$ was added in situ, as shown in Scheme 1. The condensation product, $(pddi)H_2$, was obtained via precipitation from MeOH as an off-white powder in 63% yield.[58−60]

Scheme 1. Synthesis of $(pddi)H_2$ (Ar = 2,6-$^iPr_2C_6H_3$)

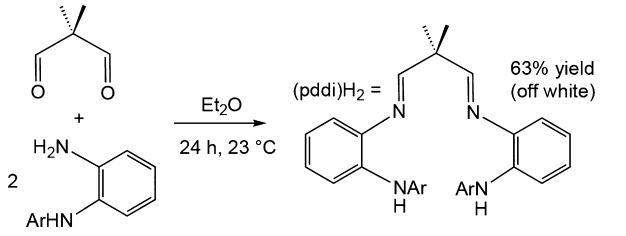

Metalations. Syntheses of (dadi)M (**1**-M; M = Cr, Fe) have already been reported via MX_2 and $(dadi)_2M'_2$ (M = Li, Na),[48,49] but generation of the anion or dianion of $(pddi)H_{(2-n)}^{-n}$ (n = 1,2) proved problematic likely due to anionic attack—either intra- or intermolecularly—at the imine, resulting in backbone cleavage despite the sterics of the CMe_2 group. Dibasic metal amides are common alternative synthons and were used with moderate success to prepare (pddi)M (**2**-M; M = Cr, Fe, and Co), as shown in Scheme 2. The complexes were all paramagnetic species with **2**-Cr showing none of the complexity of **1**-Cr, whose ground state (GS) is an S = 1 admix of S = 3/2 Cr(III) antiferromagnetically (AF) coupled to radical dadi^{3-} and S = 2 Cr(II) AF-coupled to an S = 1 excited state of (dadi^{2-})*.[48] The μ_{eff} of 4.2(1) that accorded **2**-Cr, measured via the Evans method,[61] suggests some attenuation from spin-only S = 2 (μ_{SO} = 4.9) from orbital and spin-orbit effects. Iron derivative **2**-Fe has a μ_{eff} of 4.8(1), consistent with an S = 2 center, and cobalt species **2**-Co has a μ_{eff} of 3.7(1). While this normally would be attributed to an S = 3/2 Co(II) species, typical Co orbital and spin-orbit interactions afford values far in excess of μ_{SO} = 3.9.[62,63] In combination with relatively short d(CoN) values, as indicated in the structure data below, Co exists in an S = 1/2 state.[64−66] Moreover, no EPR signal was observed for **2**-Co at 10, 77, and 298 K, prompting reevaluation of all spectroscopic and structural data in case serendipitous reduction to Co(I) occurred. No support for Co(I) was observed; hence, it is plausible that spin relaxation in the Co(II) system may be exceedingly fast.

Structures of (pddi)M (M = Cr, Fe, and Co). Single crystal x-ray diffraction studies were conducted on (pddi)M (M = Cr, Fe, and Co), molecular views of the molecules are shown in Figure 8, and selected metric parameters are given in Table 1. The molecules are all pseudo square planar, but **2**-Fe shows considerably greater core distortions than its congeners. As the first row is traversed from Cr → Fe → Co, subtle changes in covalent radii (1.18 → 1.16) might impact core metrics but the data belie such ready explanations. Chromium amide distances average 2.037(17) Å, and $d(FeN_{am})$ = 1.987(19) Å, but the related Co lengths are 1.91(4) Å, considerably shorter and indicative of a stronger field. The corresponding imine-nitrogen bonds to **2**-Cr and **2**-Fe average 2.076(9) and 2.159(37) Å, and while significantly different, they are again much longer than the corresponding bond lengths (1.931(7) Å (ave)) for **2**-Co.

Structural variations between chromium and iron stem from the distortion away from square planar in the latter case. Using Okuniewski's[67] variant of Houser's τ_4 parameter,[68] **2**-Cr has a τ_4' value of 0.41, **2**-Fe is 0.55, and **2**-Co has a value of 0.42, where τ_4' = 0 for square planar and 1 for a tetrahedron. With the constraints of a tetradentate chelate, the τ_4' parameter has limited relevance but note that the sums of the pseudo-*cis* angles for each species are **2**-Cr, 360.8°; **2**-Fe, 367.9°; and **2**-Co, 363.0°. Torquing of amide nitrogen in and out of the N_4M plane

https://doi.org/10.1021/acs.organomet.3c00197
Organometallics 2023, 42, 2747−2761

Scheme 2. Syntheses of (pddi)M (M = Cr, Fe, and Co)

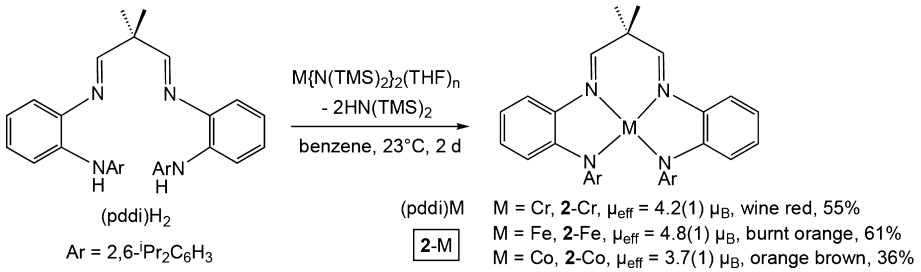

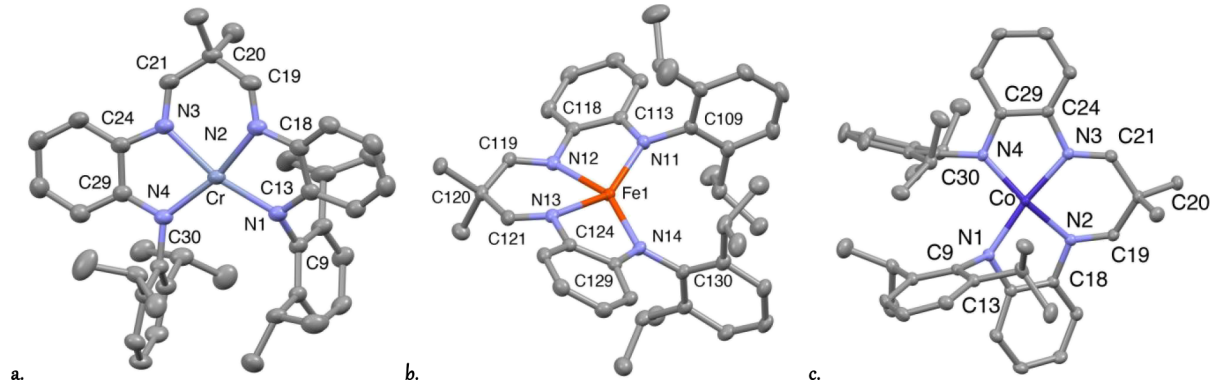

Figure 8. Molecular views of (pddi)M (**2**-M; M = Cr, Fe, and Co). One of the two statistically similar molecules in the asymmetric unit is shown for **2**-Fe. Note that the related atom labels for **2**-Fe are N(10 + #) and C(100 + #).

is the crucial source of distortion, and the splay of the N1−M−N4 angle, 124.20(5)° for **2**-Fe vs 111.83(6)° for **2**-Cr and 103.04(5)° for **2**-Co, reveals it best. Square planar geometry is electronically preferred for HS d^4 species, thereby rationalizing the minimal distortion in **2**-Cr, but HS d^6 **2**-Fe has no preference; hence, significant distortion toward tetrahedral might be expected on steric grounds. d^7 **2**-Co (d^7) also has no electronic bias, and its lack of distortion, with its short core bond lengths, again suggests that it is $S = 1/2$.

Remarkably, while variations in the core are evident, there are virtually no noteworthy differences in any of the ligand parameters, as all metrics are consistent with the drawn bonds. The ligand is thus flexible enough to accommodate each metal without any significant strain.

Nitrosylation of (pddi)M (2-M; M = Cr, Fe, and Co). Prior to nitrosylation studies, (pddi)M (**2**-M; M = Cr, Fe, and Co) was subjected to 1 atm CO in C_6D_6 solutions. Only **2**-Co was found to bind CO (ν(CO) = 1963 cm^{-1}), but upon removal of the CO atmosphere, reversion of (pddi)CoCO (**2**-CoCO) to the starting material occurred, as shown in Scheme 3. No evidence of a carbonyl complex was found for the other congeners.

Introduction of 1 equiv NO (g) to (pddi)M (**2**-M; M = Cr, Fe, and Co) in toluene solution over a 16 h period at 23 °C resulted in brown solids corresponding to the mononitrosyls, (pddi)-MNO (**2**-MNO; M = Cr, Fe, Co). The chromium derivative (pddi)CrNO (**2**-CrNO) has an extremely low ν(NO) = 1620 cm^{-1}, consistent with significant backbonding, indicative of a low charge state ($c_{NO} = -0.76$ from eq 3).

In corroboration, its μ_{eff} of 1.6(1) suggests an S_T of 1/2, likely arising from an $S = 3/2$ Cr(III) center antiferromagnetically AF coupled to an NO^- anion ($S = 1$).[23] Alternatively, NO binding might induce a core change to $S = 1$, which could AF-couple to NO radicals. In support of either case, its EPR spectrum shown in Figure 9 is consistent with a slightly rhombic geometry ascribed to an $S = 1/2$ species.

The iron derivative, (pddi)FeNO (**2**-FeNO), has an NO stretching frequency of 1703 cm^{-1} and a corresponding charge of $c_{NO} = -0.57$ (eq 3). Evans' method measurements (C_6D_6) on independently synthesized samples afforded unusual values of 2.2(1) μ_B and 2.5(1) μ_B, prompting further spectroscopic characterization. An EPR spectrum was taken on **2**-FeNO at 10 K in MeTHF, and the spectrum shown in Figure 10 clearly indicates an $S = 3/2$ iron center with $g_x = 4.390$, $g_y = 3.590$, and $g_z = 1.990$, although the latter feature was obscured by a 1% $S = 1/2$ impurity (see SI for full spectrum).

Electromers, species with nearly energetically equal ground states (GSs), have been observed in a pyridine-imine iron bromide complex by Mössbauer spectroscopy.[70] To check on this possibility, a Mössbauer spectrum (Figure 11) was obtained for **2**-FeNO and a single doublet was observed, with a δ of 0.444(4) mm/s and ΔE_Q of 1.293(8) mm/s, parameters that are well within the range of an intermediate spin Fe(II) asymmetric core. Similar spectra were obtained at 85 and 200 K (see SI) for an independently prepared sample.

SQUID magnetometry was acquired on the same sample of **2**-FeNO, and Figure 12 reveals a XT vs T plot of an $S = 3/2$ species exhibiting zero-field splitting ($D = 6.77(2)$ cm^{-1}) and a modest contribution from temperature-independent paramagnetism (TIP). The μ_{eff} values of 3.57 at 300 K and 3.44 at 50 K are unusual because they are less than spin only ($\mu_{SO} = 3.87$). Normally, SOC contributions are positive, but it is possible that a (pddi)$Fe^{\uparrow\uparrow\uparrow\uparrow}$ ($NO^{\downarrow}$) ground state (GS), where an $S = 2$ core AF-couples to the nitrosyl radical ($S = 1/2$) to afford $S_T = 3/2$, shows a different and perhaps signature behavior.

The apparent ν(NO) of (pddi)CoNO (**2**-CoNO) of 1808 cm^{-1} reveals only a modest charge of −0.34 obtained via eq 3. Its magnetism (Evans', $\mu_{eff} = 3.7(1)$ μ_B) is more than expected for

https://doi.org/10.1021/acs.organomet.3c00197
Organometallics 2023, 42, 2747−2761

Table 1. Selected Interatomic Distances (Å) and Angles (°) in (pddi)M (2-M, M = Cr, Fe, Co) and (pddi)M(NO) (M = Cr, 2-CrNO; Fe, 2-FeNO)

	2-Cr	2-Fe[a,b]	2-Co	2-CrNO[c]	2-FeNO[d]
M−N1	2.049(15)	1.9732(11)	1.9391(11)	1.9907(11)	1.9719(10)
M−N2	2.0693(15)	2.1854(11)	1.9263(11)	2.0754(11)	2.2534(10)
M−N3	2.0822(15)	2.1330(11)	1.9359(11)	2.0832(11)	2.1540(10)
M−N4	2.0246(14)	1.9999(11)	1.8830(11)	2.0128(10)	1.9999(10)
M−N5				1.6696(11)	1.7444(11)
N5−O				1.2057(15)	1.153(6)
N1−C13	1.381(2)	1.3810(17)	1.3811(17)	1.3866(16)	1.3809(16)
N1−C9	1.432(2)	1.4269(17)	1.4365(16)	1.4315(16)	1.4256(15)
N4−C29	1.372(2)	1.3798(17)	1.3857(17)	1.3866(16)	1.3912(15)
N4−C30	1.433(2)	1.4362(16)	1.4337(17)	1.4372(16)	1.4356(15)
N2−C19	1.291(2)	1.2788(18)	1.2860(18)	1.2762(18)	1.2721(16)
N2−C18	1.427(2)	1.4290(17)	1.4302(16)	1.4321(17)	1.4181(15)
N3−C21	1.286(2)	1.2785(18)	1.2812(18)	1.2811(17)	1.2731(16)
N3−C24	1.423(2)	1.4299(17)	1.4348(16)	1.4287(16)	1.4264(16)
C19−C20	1.491(3)	1.4988(19)	1.4925(18)	1.4916(19)	1.5124(17)
C20−C21	1.492(3)	1.4960(19)	1.4916(18)	1.4942(19)	1.5152(17)
C13−C18	1.416(2)	1.4120(19)	1.4078(19)	1.4072(19)	1.4146(17)
C24−C29	1.414(2)	1.4197(18)	1.4035(19)	1.4063(18)	1.4151(17)
C19−C21	2.551(3)	2.542(2)	2.528(2)	2.545(2)	2.468(2)
N1−M−N2	80.89(6)	79.67(4)	84.10(5)	79.66(4)	77.18(4)
N1−M−N3	166.55(6)	147.49(4)	168.44(5)	148.09(5)	117.07(4)
N1−M−N4	111.83(6)	124.20(5)	103.04(5)	105.45(4)	112.48(4)
N2−M−N3	87.76(6)	83.35(4)	91.47(5)	85.83(4)	77.04(4)
N2−M−N4	165.72(11)	152.86(4)	161.86(5)	160.75(4)	156.14(4)
N3−M−N4	80.35(6)	80.63(4)	84.37(5)	80.35(4)	79.19(4)
N1−M−N5				104.71(5)	112.94(5)
N2−M−N5				90.04(5)	94.89(4)
N3−M−N5				103.55(5)	125.63(5)
N4−M−N5				106.14(5)	100.59(5)
C18−N2−C19	120.06(16)	117.71(11)	118.52(11)	119.54(11)	120.58(11)
C21−N3−C24	119.92(15)	117.42(11)	118.99(11)	118.99(11)	121.33(10)
N2−C19−C20	127.04(17)	126.07(12)	126.56(12)	126.62(12)	122.52(11)
N3−C21−C20	127.83(17)	127.93(12)	126.39(12)	128.91(12)	123.47(11)
C19−C20−C21	117.56(15)	116.18(11)	115.84(11)	116.93(12)	109.20(10)
M−N5−O				175.12(10)	158.3(7)

[a]One of the two molecules in the asymmetric unit; metric parameters between the two are statistically similar. [b]For the atom labels for 2-Fe: N(10 + #), C(100 + #). [c]d(NO) = 1.2057(15). [d]Disordered NO (∠Fe−N−OA, 158.3(7)°, ∠Fe−N−OB, 157.7(8)°; d(N5−OA) = 1.153(6), and d(N5−OB) = 1.163(6)).

an $S = 3/2$ center AF-coupled to a nitrosyl radical ($S_T = 1$), but Co can manifest large orbital and spin-orbit contributions.[62,63] In this case, the data must be considered tentative for pure 2-CoNO. Although IR spectra obtained soon after synthesis have similar fingerprint regions to the chromium and iron congeners, color changes have been noted while preparing samples. Its sensitivity reveals more than just NO loss, as pddi degradation is facile. Attempts to crystallize 2-CoNO instead led to the isolation of $\{[N,N,N,O\text{-}1,2\text{-}ArNC_6H_4N{=}CHCMe_2NO]Co\}_2$ (3; Ar = 2,6-^{i}Pr$_2$C$_6$H$_3$). Loss of a "CNC_6H_4NAr" fragment is incurred during pddi degradation concomitant with insertion of an NO radical[71] and dimerization. Dimer 3 is diamagnetic (Evans'), although the ^{1}H NMR resonances are somewhat broad, and as the metrics and calculations suggest, each Co center is $S = 1/2$ AF-coupled to the N,O-alkylnitrosyl radical bridge.

Structures of (pddi)MNO (2-MNO; M = Cr and Fe). Shown in Figure 13 are molecular views of (pddi)CrNO (2-CrNO, a) and (pddi)FeNO (2-FeNO, b), whose selected metric parameters are listed alongside those of 2-M in Table 1. 2-CrNO is pseudo square pyramidal with an Addison parameter[72] of $\tau = 0.21$, with the nitrosyl in the apical position. The NO is tilted somewhat toward imine nitrogen N2 (∠N2−Cr−N5 = 90.04(5)°), whereas the remaining nitrosyl nitrogen to basal angles ranges from 103.55° to 106.14(5)°. The Cr−N−O angle is 175.12(0)°, and the chromium-nitrogen distance is quite short at 1.6696(11) Å, consistent with significant backbonding to linear nitrosyl. Binding of NO to Cr has hardly changed the remaining core distances, which average 2.040(45) Å compared to 2.056(25) Å (ave) for 2-Cr. In addition, various distances within the chelate are also essentially unperturbed.

Iron derivative (pddi)FeNO (2-FeNO) is less regular, with an Addison parameter[72] of $\tau = 0.49$, indicative of an intermediate coordinate geometry between a square pyramid ($\tau = 0.00$) and tbp ($\tau = 1.00$), despite constraints of the chelate. The nitrosyl nitrogen to basal nitrogen angles corroborate the inconclusive τ values as 94.89(4)° and 100.59(4)°, and the remaining ones are 112.94(5)° and 125.63(5)°. Core iron-nitrogen distances are largely unaffected by the nitrosyl except imine-N2, which has lengthened by 0.068 Å over the corresponding distance in 2-Fe.

https://doi.org/10.1021/acs.organomet.3c00197
Organometallics 2023, 42, 2747−2761

Scheme 3. Reversible Carbonylation of 2-Co to (pddi)CoCO (2-CoCO), Nitrosylation of 2-M (M = Cr, Fe, and Co) to (pddi)MNO (2-MNO; M = Cr, Fe, Co), and the Co Degradation Product, 3

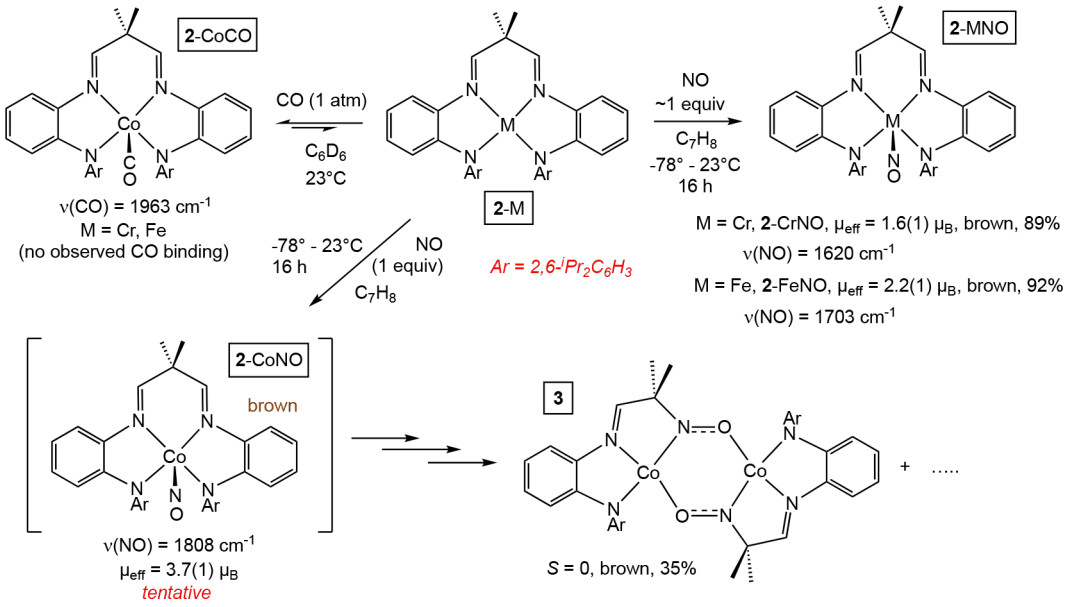

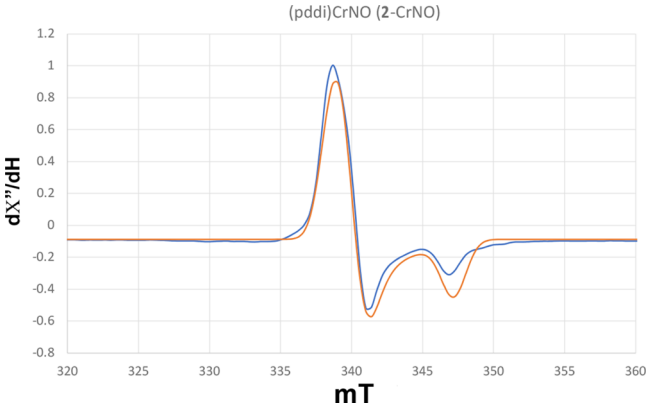

Figure 9. EPR spectrum of (pddi)CrNO (**2**-CrNO; blue) at 10 K in toluene (fit (red)): g_x = 1.998, g_y = 1.948, g_z = 1.988.

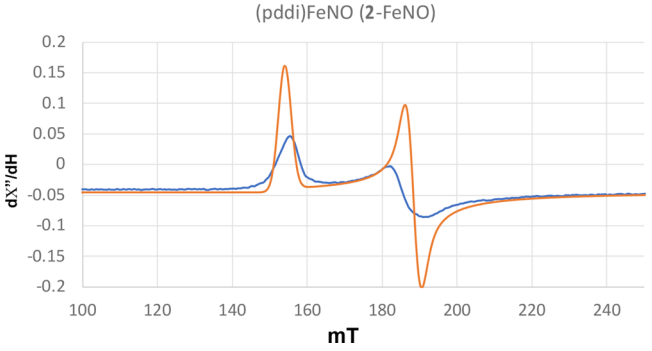

Figure 10. Partial EPR spectrum of (pddi)FeNO (**2**-FeNO; blue) at 10 K in MeTHF showing an S = 3/2 species (fit (orange): g_1 = 4.390, g_2 = 3.590, g_3 = 1.990). The low field component (not shown) is obscured by a 1% S = 1/2 impurity. See the SI (Figure S7) for the full spectrum.

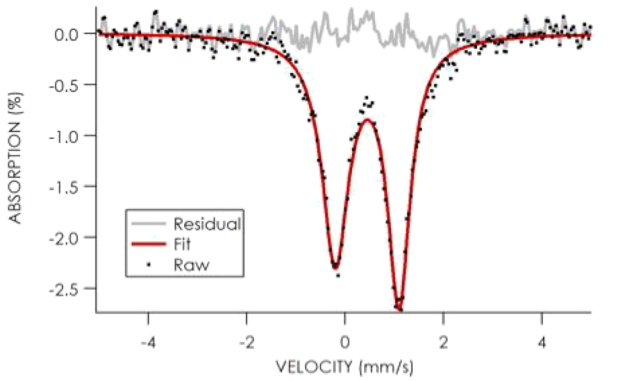

Figure 11. Mössbauer spectrum obtained for **2**-FeNO at 85 K and 0 field (black dots; fit (red)): δ = 0.444(5) mm/s; ΔE_Q = 1.293(8) mm/s, Γ_L = 0.654(15) mm/s, Γ_R = 0.555(12) mm/s. A second sample taken at 85 and 200 K (0 field) manifests similar parameters; see Supplemental Information.

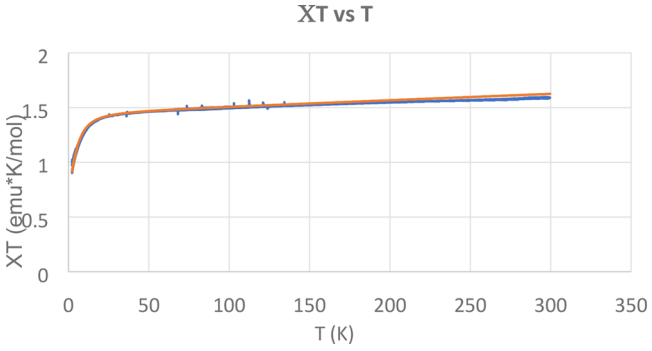

Figure 12. SQUID magnetometry measurement (XT vs T(K)) of (pddi)FeNO (**2**-FeNO, same sample as in Figure 10) showing an S = 3/2 species (μ_{eff} = 3.57 at 300 K; 3.44 at 50 K). Fit (orange) parameters are g_{iso} = 1.7681(2); D = 6.77(2) cm^{-1}; and TIP = 0.58 × 10^{-3}(0.17 × 10^{-5}).

Again, no significant differences are apparent within the chelate between the 4- and 5-coordinate species. The nitrosyl is bent at a 158.3(7)° angle, a value within the standard window of neutral NO ligation. While there is no structural preference for a d^6 intermediate spin species from a σ-bonding standpoint, there may be a more favorable AF-coupling from orbitals with π-

https://doi.org/10.1021/acs.organomet.3c00197
Organometallics 2023, 42, 2747−2761

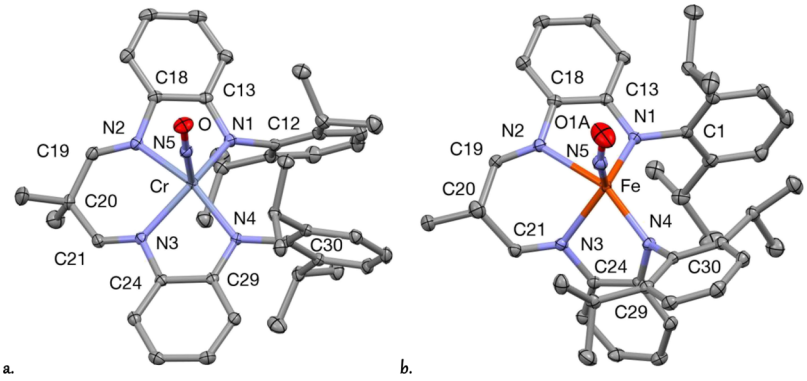

Figure 13. Molecular views of (pddi)MNO (**2**-MNO; M = Cr (a) and Fe (b)).

symmetry, potentially a consideration when rationalizing severe distortion.

Structure of {[κ^3-N,N,N-1,2-ArNC$_6$H$_4$N=CHCMe$_2$NO]-Co}$_2$ (3). The dicobalt dimer {[κ^3-N,N,N-1,2-ArNC$_6$H$_4$N=CHCMe$_2$NO]Co}$_2$ (**3**) is remarkably flat (sum of core angles = 360.05°) compared to its precursors, and the pseudo-square planar Co centers are related by inversion symmetry (Figure 14). Related core distances are ∼0.06 Å shorter than that in

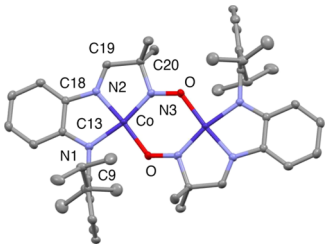

Figure 14. Molecular view of {[κ^3-N,N,N-1,2-ArNC$_6$H$_4$N=CHCMe$_2$NO]Co}$_2$ (**3**). Selected interatomic distances (Å) and angles (°): CoCo, 3.634, CoO, 1.8607(12); Co−N1, 1.8719(15); Co−N2, 1.8612(15); Co−N3, 1.7737(15); N1−C9, 1.424(2); N1−C13, 1.377(2); C13−C18, 1.411(2); N2−C18, 1.417(2); N2−C19, 1.286(2); C19−C20, 1.492(2); N3−C20, 1.507(2); N3−O, 1.3131(19); O−Co−N1, 90.45(6); O−Co−N2, 174.63(6); O−Co−N3, 100.52(6); N1−Co−N2, 84.60(6); N1−Co−N3, 168.96(6); N2−Co−N3, 84.48(6).

(pddi)Co (**2**-Co), and the N−O distance of 1.3131(19) Å is between single (∼1.40 Å) and double (∼1.24 Å) bond lengths, close to that of a neutral radical nitroxyl species (1.30 Å).[69] In consideration of the metrics, **3** may be best described as formally LS Co(II) AF-coupled to a radical alkylnitroso-anion bridge.

Calculations. (pddi)M (2-M; M = Cr, Fe, Co). Using crystal structure geometries as starting points, (pddi)M (**2**-M, M = Cr, Fe, Co) was calculated using the hybrid functional ωB97xD and the pure functional BP86 for comparison, leading often to disparate results. As simple coordination compounds with magnetic measurements indicative of the expected high spin configurations, calculations of **2**-Cr and **2**-Fe conducted using ωB97xD afforded the expected quintet GSs. The disposition of spin density was similar for both functionals regarding **2**-M, largely centered on the metals, with only modest spin density on the pddi ligand. MCSCf calculations suggested minimal multi-reference behavior as judged by natural orbital occupation numbers (NOONs) for the predicted GSs of (pddi)M (**2**-M, M = Cr and Fe). The natural orbitals of (pddi)Fe (**2**-Fe) are given in the Supporting Information (Figure S8), including occupation numbers showing a classic high spin system; orbitals for **2**-Cr are similarly defined.

Unfortunately, the geometry of **2**-Co was also calculated to be a quartet, but the core geometry Co-N distances were all ∼0.1 Å longer than the experiment. While the quartet GS is seemingly supported by a μ_{eff} of 3.7(1) μ_B, it is rare that Co does not exhibit much higher than μ_{SO} values due to orbital and spin-orbit contributions.[62,63] Employment of BP86 predicted the quintet GS for **2**-Cr and an intermediate spin triplet for **2**-Fe and did provide a doublet geometry for **2**-Co that was in very good agreement with crystal structure determination. Figure 15

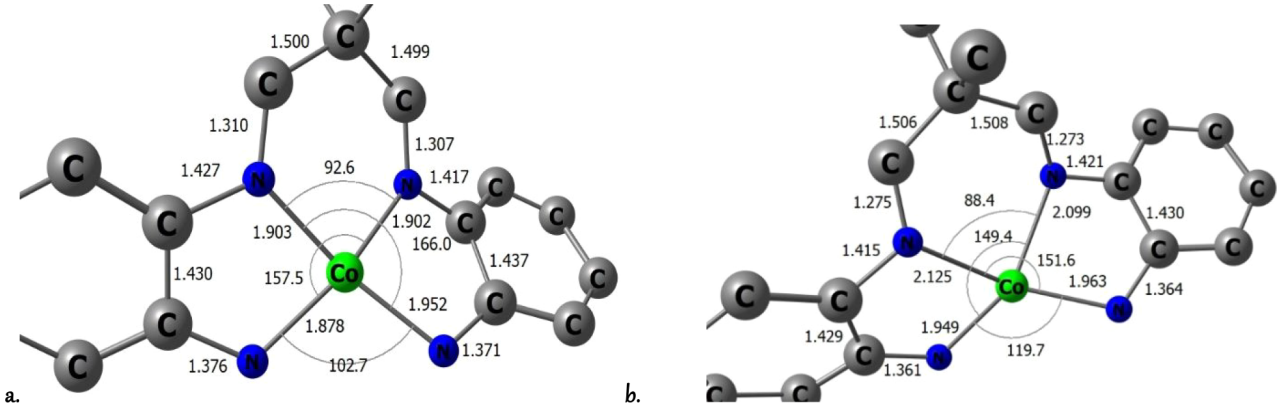

Figure 15. Doublet (a) and quartet (b) core geometries of (pddi)Co (**2**-Co; the 2,6-^{i}PrC$_6$H$_3$ were replaced with H). Calculations are at the BP86/def2svp:UFF level.

https://doi.org/10.1021/acs.organomet.3c00197
Organometallics 2023, 42, 2747−2761

illustrates the BP86 calculated geometries of both the doublet and quartet GSs of **2**-Co, showing the rough ∼0.1 Å difference in core distances between the HS and LS states.

Figure 16 illustrates the frontier orbitals of (pddi)Co (**2′**-Co; the 2,6-^{i}PrC$_6$H$_3$ were replaced with H) and reveals the

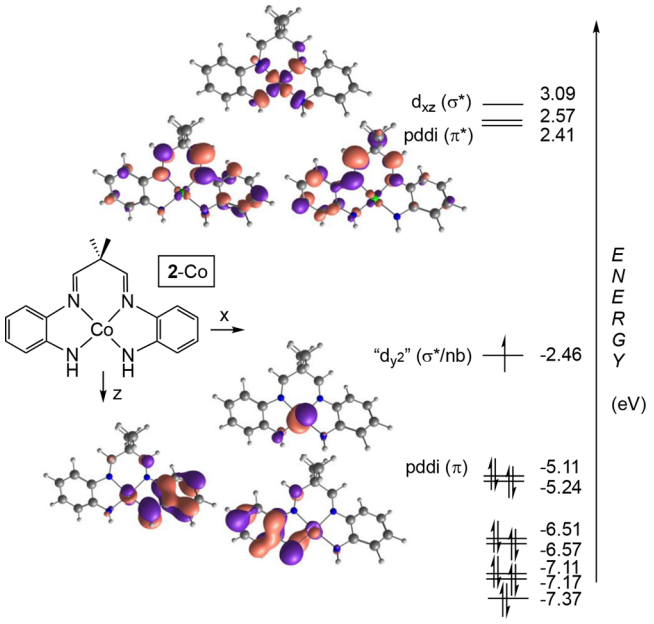

Figure 16. Kohn-Sham frontier orbitals of (pddi)Co (**2′**-Co; the 2,6-^{i}PrC$_6$H$_3$ were replaced with H) calculated at the BP86/def2svp:UFF level. The energies should be considered relative only. The orbitals below −5.24 eV are d- and admixtures of d/pddi.

discrepancy between the ωB97xD/def2svp:UFF and BP86/def2svp:UFF functionals. The levels of calculation clash in their handling of the weak π-interactions encountered in first row metals and heterocycles, predominantly N-based, whereas the former functional underestimates any metal−ligand π-bonding/antibonding, rendering **2**-Co a high spin complex akin to its chromium and iron congeners; the latter functional over-accounts for it. Note that the widely spread energies of the frontier orbitals are not likely to be accurate and must be interpreted as simply showing their relative order, but the geometry is reasonable, and the magnetism can still be rationalized. Both sets of LUMOs and doubly filled bonding orbitals are largely ligand based.

(pddi)CrNO (2-CrNO). Shown in Figure 17 is the ωB97xD/def2svp:UFF optimized core geometry of (pddi)CrNO (**2**-CrNO), which corresponds to a doublet that is 3.4 kcal/mol lower in free energy than the quartet. The d(CrN) of the nitrosyl is 1.694 Å, a reasonable match to the experimental 1.6696(11) Å and the corresponding bond angle is calculated to be 175.5°, which closely matches the 175.12(10)° obtained from XRD. The quartet geometry has a significantly bent nitrosyl (159.9°) and a chromium-nitrogen bond length ∼0.1 Å greater than experiment (1.789 Å). Mulliken spin densities for the doublet are consistent with antiferromagnetic (AF) coupling between intermediate spin Cr(II) and neutral NO, that is, (pddi^{2-})-Cr$^{2+(\uparrow\downarrow\uparrow\uparrow)}NO^{(\downarrow)}$, consistent with the EPR spectrum. The higher energy quartet state is similarly described as a high spin Cr(II) core that is AF-coupled to neutral NO, that is, (pddi^{2-})-Cr$^{2+(\uparrow\uparrow\uparrow\uparrow)}NO^{(\downarrow)}$.

(pddi)FeNO (2-FeNO). Calculations on (pddi)FeNO (**2**-FeNO) show the difficulties of obtaining accuracy on open-shell systems complicated by a radical ligand. Table 2 shows that the

Table 2. Selected Experimental and Calculated Fe-NO Metric Parameters for (pddi)FeNO (2-FeNO)

functional/Expt	2S + 1	d(FeN)	d(NO)	/FeNO
ωB97xD	2	1.738	1.163	160.1
ωB97xD	4	1.789	1.167	159.9
BP86	2	1.652	1.183	160.1
BP86	4	1.691	1.182	157.7
XRD[a]		1.744	1.152	158.3
XRD[a]		1.744	1.163	157.5

[a]Disordered nitrosyl affords two similar sets of parameters.

geometry of **2**-FeNO is well described by the functional that proved most accurate for **2**-CrNO (ωB97xD/def2svp:UFF), but this doublet is calculated to be ∼0.5 eV above the corresponding quartet. The doublet is best described as (pddi^{2-})Fe$^{2+(\uparrow\downarrow\uparrow\uparrow)}NO^{(\downarrow)}$, and the quartet is also analogous to the previous chromium compound as (pddi^{2-})Fe$^{2+(\uparrow\uparrow\uparrow\uparrow)}NO^{(\downarrow)}$. Use of the pure functional BP86 affords similar GS descriptions of doublet and quartet states, but now, the S = 1/2 GS is only slightly favored by −0.3 kcal/mol. Recall that the Evans' method

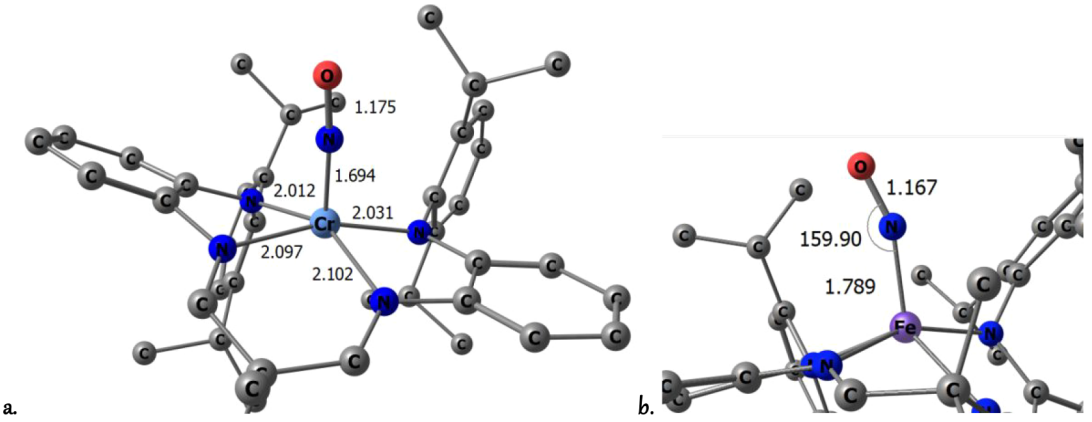

Figure 17. (a) Doublet core geometry of (pddi)CrNO (2-NO, ∠CrNO = 175.5°) suggests antiferromagnetic (AF) coupling between intermediate spin Cr(II) and neutral NO, that is, (pddi^{2-})Cr$^{2+(\uparrow\downarrow\uparrow\uparrow)}NO^{(\downarrow)}$. (b) Truncated geometry of energetically nearby (+3.4 kcal/mol) quartet state featuring high spin Cr(II) AF-coupled to neutral NO, that is, (pddi^{2-})Cr$^{2+(\uparrow\uparrow\uparrow\uparrow)}NO^{(\downarrow)}$. Calculations are at the ωB97xD/def2svp:UFF level.

https://doi.org/10.1021/acs.organomet.3c00197
Organometallics 2023, 42, 2747−2761

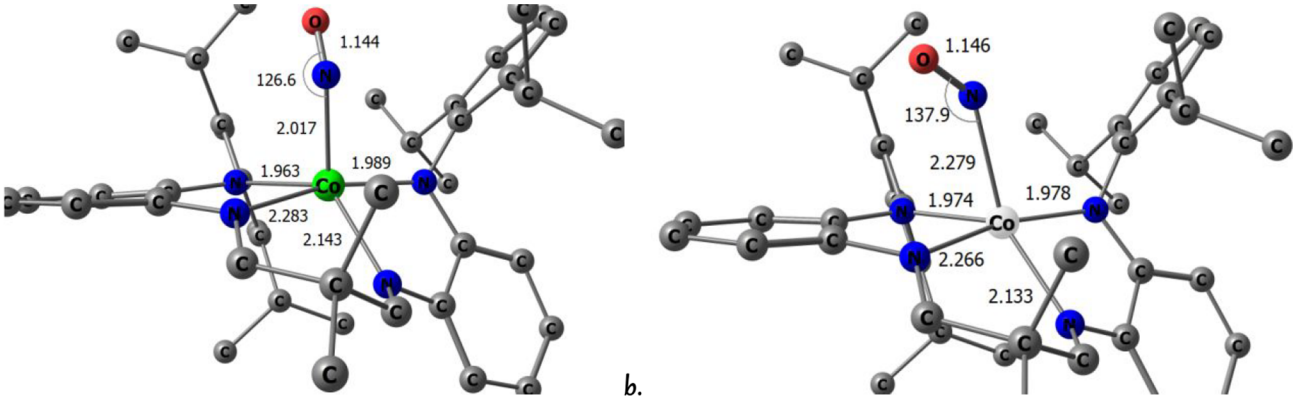

Figure 18. (a) Triplet core geometry of highly distorted (pddi)CoNO (2-NO) suggests antiferromagnetic (AF) coupling between $S = 3/2$ Co(II) and neutral NO, that is, $(pddi^{2-})Co^{2+(\uparrow\uparrow\uparrow)}NO^{(\downarrow)}$. (b) Truncated geometry of a quintet state featuring HS Co(III) and a bent, diamagnetic NO anion, that is, $(pddi^{2-})Co^{3+(\uparrow\uparrow\uparrow\uparrow)}NO^{(-)}$. Calculations are at the B97xD/def2svp:UFF level.

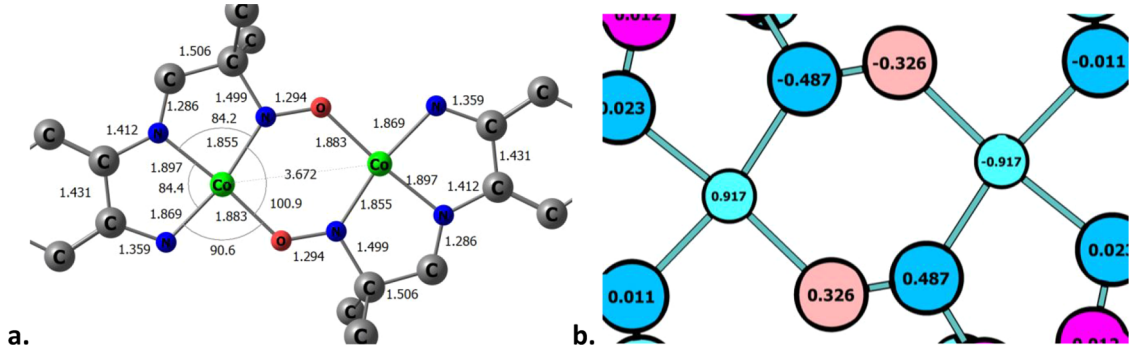

Figure 19. Calculated core (a) of the lowest singlet state of $\{[\kappa^3\text{-N,N,N-1,2-HNC}_6\text{H}_4\text{N=CHCMe}_2\text{NO}]\text{Co}\}_2$ (**3′**, the 2,6-^{i}PrC$_6$H$_3$ was replaced with H) and (b) core charge delocalization from broken symmetry. Calculations were at the B3Lyp/def2svp/SMD-HF level.

measurement of **2**-FeNO showed $\mu = 2.2\ (1)\ \mu_B$, which could be construed as a mixture of doublet and quartet states. This conjecture was not supported by the Mössbauer study, but the former is a solution measurement, and the latter is from the crystalline material. While the energetics are best approximated by BP86, assessment of the critical metrics is poor compared to ωB97xD/def2svp:UFF.

(pddi)CoNO (2-CoNO). Crystal growth suitable for X-ray analysis of (pddi)CoNO (**2**-CoNO) has been fraught with competition from degradation; hence calculations were necessary to assess this species. Here, the correlation of d(MN) and d(NO) with the 1808 cm^{-1} stretching frequency can be used as a rough approximation, and a d(NO) of ∼1.15 Å is predicted, with only a small likelihood of bent nitrosyl. Unfortunately, calculations have failed to produce solutions that are completely satisfactory.

In Figure 18, a calculated distorted triplet state of **2**-CoNO, that is, $(pddi^{2-})Co^{2+(\uparrow\uparrow\uparrow)}NO^{(\downarrow)}$, where HS Co(II) is AF-coupled to neutral NO, affords a nitrosyl with a severely bent CoNO angle of 126.6°. A quintet state in which a bent nitrosyl anion is bound to a high spin Co(III) center, that is, $(pddi^{2-})Co^{3+(\uparrow\uparrow\uparrow\uparrow)}NO^{(-)}$, is unlikely given its substantially higher energy and failure to rationalize its magnetism.

The core metrics of the triplet appear reasonable, and it is expected that in binding NO, reversion to high spin Co(II) may occur as d_{z2} is raised in energy. Occupation of this orbital by 1e$^-$, which is antibonding with respect to NO sigma donation, may cause the nitrosyl to bind weakly as the radical, hence the modest backbonding. While the scaled calculated ν(NO) of 1880 cm^{-1} does not quite mimic the experimental value of 1808 cm^{-1}, it is within reason. The $S = 1$ GS is consistent with magnetism (3.7(1) μ_B), provided there is no orbital or spin-orbit contribution, but this would be unusual for Co(II); hence, the aforementioned lability of NO and dppi degradation are likely to be affecting the accuracy of the measurement.

$\{[\kappa^3$-N,N,N-1,2-ArNC$_6$H$_4$N=CHCMe$_2$NO]Co$\}_2$ (3). Calculations on $\{[\kappa^3\text{-N,N,N-1,2-HNC}_6\text{H}_4\text{N=CHCMe}_2\text{NO}]\text{Co}\}_2$ (**3′**, the 2,6-^{i}PrC$_6$H$_3$ was replaced with H) corroborate its $S = 0$ GS, and as expected from the metrical parameters, specifically d(NO), it is not Co(III). Figure 19a shows a very good correspondence between the experimental core described in the caption of Figure 13 and the calculated values, showing the short distances attributable to a suitably strong ligand field. The 1.294 Å nitrogen-oxygen distance is best rationalized as a radical alkylnitroso-anion that is AF-coupled to Co(II), affording the formulation of **3** as a LS $[(LX^-)Co^{2+(\uparrow)}RNO^{(-\downarrow)}][(LX^-)Co^{2+(\downarrow)}RNO^{(-\uparrow)}]$ center. Nearby in energy (∼1 kcal/mol) is the related LS $[(LX^-)Co^{2+(\uparrow)}RNO^{(-\downarrow)}][(LX^-)Co^{2+(\uparrow)}RNO^{(-\downarrow)}]$ configuration, where the pertinent spins on one half of the molecule are flipped. In support of this formulation, broken symmetry calculations shown in Figure 18b reveal unpaired spin densities of 0.917 on Co and 0.487 and 0.326 (0.813 total) of opposite sign on the alkylnitroso bridge, corresponding to roughly 1e$^-$ on each.

CONCLUSIONS

The research above serves to augment the long history of the nitrosyl ligand in organometallic and inorganic chemistry and

https://doi.org/10.1021/acs.organomet.3c00197
Organometallics 2023, 42, 2747−2761

hopefully continues to dispel notions that electron counting methods of the former are electronically realistic, as plenty of previous investigators have also intimated.[1−9,11−27,30−33,40] Reliance on valence bond theory and formal oxidation states plays into the difficulties in assessing an appropriate charge to an NO ligand that is intrinsically electronegative in comparison to its metal binder. It is probably best to consider NO as neutral or anionic when linear and anionic when bent in conforming to the estimated atomic number (EAN) rule, that is, the 18 e^- rule.

The partitioning of charge in molecular orbital descriptions is method dependent, but CDVR is a benchtop means of estimation that is a swift pedagogical aid. The use of CDVR, a means of *relative* charge assessment, provides no evidence that NO should be construed as having a net positive charge, and it can be a π-backbonding ligand under any circumstance. It is conceivable that inverted ligand fields[73] might provide a charge inversion, but it is doubtful that NO would bind in these circumstances. The survey also emphasizes the folly of using ν(NO) to distinguish bent from linear configurations of NO, but the use of the 18 e^- rule may aid in distinguishing the two modes.

The tetradentate ligand $pddi^{2-}$ is introduced here as a means of making discrete nitrosyl derivatives from nitrosylation of (pddi)M (**2**-M; M = Cr, Fe, Co). Five coordinate (pddi)MNO (**2**-MNO; M = Cr, Fe, Co) affords adducts with ν(NO) commensurate with their CDVR charge states (c_{Cr} = 2.6, 1620 cm^{-1}; c_{Fe} = 2.0, 1703 cm^{-1}; c_{Co} = 1.6, 1808 cm^{-1}), consistent with the expected degree of backbonding. High level calculations showcase the difficulties of interpreting open shell systems complicated by inclusion of an odd electron ligand. Certain functionals gave satisfactory electronic structures for **2**-M and **2**-MNO for Cr and Fe, but there is some consternation regarding choosing a functional simply because it applies. Nonetheless, GSs where d_{z2} is unoccupied prevail for **2**-CrNO and **2**-FeNO, a crucial feature as commented upon by Parkin.[27] Calculations of **2**-Co and **2**-CoNO also proved difficult, as approaches to these first row TM species suffer from difficulties of handling of weak π-interactions, especially with N-donors. It was gratifying that the diamagnetism of $\{[\kappa^3$-N,N,N-1,2-$ArNC_6H_4N{=}CHCMe_2NO]Co\}_2$ (**3**), was readily handled via numerous functionals.

Investigations of CDVR in these laboratories reveal that amides have typical charges of −0.75(5), hence it was expected that (pddi)M (**2**-M; M = Cr, Fe) would produce stable (pddi)MNO (**2**-MNO) and reflect the degree of backbonding via ν(NO). Charges accorded the nitrosyls **2**-CrNO (c_{NO} = −0.87) and **2**-FeNO (c_{NO} = −0.68) fit the paradigm, but the c_{NO} = −0.43 for the nitrosyl of **2**-CoNO, summed with the two amides (minimum ∼ (−1.40)), is on the cusp of being commensurate with the c_{Co} of +1.6. As a consequence, this serves as an example of how CDVR can predict instability.

■ ASSOCIATED CONTENT

Supporting Information

The Supporting Information is available free of charge at https://pubs.acs.org/doi/10.1021/acs.organomet.3c00197.

Experimental details; computations; and X-ray crystal structures (PDF)

Calculations of complexes (XLSX)

Calculations of complexes (XLSX)

Calculations of complexes (XLSX)

Calculations of complexes (XLSX)

Accession Codes

CCDC 2258800−2258805 contain the supplementary crystallographic data for this paper. These data can be obtained free of charge via www.ccdc.cam.ac.uk/data_request/cif, or by emailing data_request@ccdc.cam.ac.uk, or by contacting The Cambridge Crystallographic Data Centre, 12 Union Road, Cambridge CB2 1EZ, UK; fax: +44 1223 336033.

■ AUTHOR INFORMATION

Corresponding Author

Peter T. Wolczanski − *Department of Chemistry and Chemical Biology, Baker Laboratory, Cornell University, Ithaca, New York 14853, United States;* orcid.org/0000-0003-4801-0614; Email: ptw2@cornell.edu

Authors

Alexander A. D'Arpino − *Department of Chemistry and Chemical Biology, Baker Laboratory, Cornell University, Ithaca, New York 14853, United States;* orcid.org/0000-0003-0991-096X

Thomas R. Cundari − *Department of Chemistry, CasCam, University of North Texas, Denton, Texas 76201, United States;* orcid.org/0000-0003-1822-6473

Samantha N. MacMillan − *Department of Chemistry and Chemical Biology, Baker Laboratory, Cornell University, Ithaca, New York 14853, United States;* orcid.org/0000-0001-6516-1823

Complete contact information is available at: https://pubs.acs.org/10.1021/acs.organomet.3c00197

Notes

The authors declare no competing financial interest.

■ ACKNOWLEDGMENTS

PTW and TRC acknowledge the National Science Foundation for funding this work (CHE-1953884, CHE-1953547, and CHE-1531468) and the support of Cornell University. Values pertaining to NO^n (n = +, 0, −) are taken from NIST (webbook.nist.gov.chemistry/). We thank Prof. Kyle M. Lancaster, Melissa M. Bollmeyer, Mary C. Eaton, Tyler Azbell, and Robert W. Voland for aid in obtaining EPR, SQUID, and Mössbauer measurements. EPR studies reported in this publication were supported by the National Institute of General Medical Sciences of the National Institutes of Health under Award Number 1R24GM146107. The authors declare no competing financial interests.

■ REFERENCES

(1) (a) Pauling, L. *The Nature of the Chemical Bond*, 3rd ed.; Cornell University Press: Ithaca, NY, USA, 1960. (b) Pauling, L. The Modern Theory of Valency. *J. Chem. Soc.* **1948**, 1461−1467.

(2) Aullón, G.; Alvarez, S. Oxidation States, atomic charges and orbital populations in transition metal complexes. *Theor. Chem. Acc.* **2009**, *123*, 67−73.

(3) Cioslowski, J.; Hay, P. J.; Ritchie, J. P. Charge Distributions and Effective Atomic Charges in Transition-Metal Complexes Using Generalized Atomic Polar Tensors and Topological Analysis. *J. Phys. Chem.* **1990**, *94*, 148−151.

(4) Steinborn, D. The Concept of Oxidation States in Metal Complexes. *J. Chem. Educ.* **2004**, *81*, 1148−1154.

(5) Karen, P. Oxidation state, a long standing issue! *Angew. Chem., Int. Ed.* **2015**, *54*, 4716−4726.

(6) (a) Raebiger, H.; Lany, S.; Zunger, A. Charge self-regulation upon changing the oxidation state of transition metals in insulators. *Nature*

2008, *435*, 763−766. (b) Resta, R. Charge states in transition. *Nature* **2008**, *453*, 735.
(7) (a) Weinhold, F.; Landis, C. R.; Glendening, E. D. What is NBO analysis and how is it useful? *Int. Rev. Phys. Chem.* **2016**, *35*, 399−440. (b) Weinhold, F.; Landis, C. R. *Discovering Chemistry with Natural Bond Orbitals*; Wiley: Hoboken, NJ, USA, 2012.
(8) (a) Mortier, W. J.; Leuven, K. U. Electronegativity equalization and its applications. *Struct. Bondings* **1987**, *66*, 125−143. (b) Mortier, W. J.; Ghosh, S. K.; Shankar, S. Electronegativity Equalization Method for the Calculation of Atomic Charges in Molecules. *J. Am. Chem. Soc.* **1986**, *108*, 4315−4320.
(9) Mitoraj, M. P.; Michalak, A.; Ziegler, T. A Combined Charge and Energy Decomposition Scheme for Bond Analysis. *J. Chem. Theory Comput.* **2009**, *5*, 962−975.
(10) (a) Richter-Addo, G. B.; Legzdins, P. *Metal Nitrosyls*; Oxford University Press: New York, 1992. (b) Richter-Addo, G. B.; Legzdins, P.; Burstyn, J. Introduction: Nitric oxide chemistry. *Chem. Rev.* **2002**, *102*, 857−860. (c) Eisenberg, R.; Meyer, C. D. Coordination Chemistry of Nitric Oxide. *Acc. Chem. Res.* **1975**, *8*, 26−34.
(11) Hartwig, J. F. *Organotransition Metal Chemistry*; University Science Books: Mill Valley, CA, 2010.
(12) Mingos, D. M. P.; Sherman, D. J. Transition-Metal Nitrosyl Complexes. *Adv. Inorg. Chem.* **1989**, *34*, 293−377.
(13) De La Cruz, C.; Sheppard, N. A Structure-Based Analysis of the Vibrational Spectra of Nitrosyl Ligands in Transition-Metal Coordination Complexes and Clusters. *Spectrochim. Acta, Part A* **2011**, *78*, 7−28.
(14) Lewandowska, H. Spectroscopic Characterization of Nitrosyl Complexes. In *Nitrosyl Complexes in Inorganic Chemistry, Biochemistry and Medicine I*; Mingos, D. M. P., Ed.; Springer Berlin Heidelberg: Berlin, Heidelberg, 2013; pp 115−165.
(15) Holloway, L. R.; Li, L. The Preparation, Structural Characteristics, and Physical Chemical Properties of Metal-Nitrosyl Complexes. *Struct. Bonding* **2013**, *154*, 53−98.
(16) Balcells, D.; Carbó, J. J.; Maseras, F.; Eisenstein, O. Self-Consistency versus "Best-Fit" Approaches in Understanding the Structure of Metal Nitrosyl Complexes. *Organometallics* **2004**, *23*, 6008−6014.
(17) Enemark, J. H.; Feltham, R. D. Principles of structure, bonding, and reactivity for metal nitrosyl complexes. *Coord. Chem. Rev.* **1974**, *13*, 339−406.
(18) Lu, T.-T.; Weng, T.-C.; Liaw, W.-F. X-ray Emission Spectroscopy: A Spectroscopic Measure for the Determination of NO Oxidation States in Fe-NO Complexes. *Angew. Chem., Int. Ed.* **2014**, *53*, 11562−11566.
(19) Yan, J. J.; Gonzales, M. A.; Mascharak, P. K.; Hedman, B.; Hodgson, K. O.; Solomon, E. I. L-Edge X-ray Absorption Spectroscopic Investigation of $\{FeNO\}^6$: Delocalization vs Antiferromagnetic Coupling. *J. Am. Chem. Soc.* **2017**, *139*, 1215−1225.
(20) Phu, P. N.; Gutierrez, C. E.; Kundu, S.; Sokaras, D.; Kroll, T.; Warren, T. H.; Stieber, S. C. E. Quantification of Ni-N-O Bond Angles and NO Activation by X-ray Emission Spectroscopy. *Inorg. Chem.* **2021**, *60*, 736−744.
(21) Sharp, D. W. A.; Thorley, J. The Infrared Spectrum of the Nitrosonium Ion. *J. Chem. Soc.* **1963**, 3557−3560.
(22) Arrington, C. A.; Dunning, T. H., Jr.; Woon, D. E. Electron Affinity of NO. *J. Phys. Chem. A* **2007**, *111*, 11185−11188.
(23) Tomson, N. C.; Crimmin, M. R.; Petrenko, T.; Rosebrugh, L. E.; Sproules, S.; Boyd, W. C.; Bergman, R. G.; DeBeer, S.; Toste, F. D.; Wieghardt, K. A Step beyond the Feltham−Enemark Notation: Spectroscopic and Correlated *ab initio* Computational Support for an Antiferromagnetically Coupled M(II)−$(NO)^-$ Description of Tp*M-(NO) (M = Co, Ni). *J. Am. Chem. Soc.* **2011**, *133*, 18785−18801.
(24) Ampßler, T.; Monsch, G.; Popp, J.; Riggenmann, T.; Salvador, P.; Schröder, D.; Klüfers, P. Not Guilty on Every Count: The "Non-Innocent" Nitrosyl Ligand in the Framework of IUPAC's Oxidation-State Formalism. *Angew. Chem., Int. Ed.* **2020**, *59*, 12381−12386.
(25) Popp, J.; Riggenmann, T.; Schröder, D.; Ampßler, T.; Salvador, P.; Klüfers, P. Bent and Linear $\{CoNO\}^8$ Entities: Structure and Bonding in a Prototypic Class of Nitrosyls. *Inorg. Chem.* **2021**, *60*, 15980−15996.
(26) Fujisawa, K.; Soma, S.; Kurihara, H.; Dong, H. T.; Bilodeau, M.; Lehnert, N. *Dalton Trans.* **2017**, *46*, 13273−13289.
(27) Landry, V. K.; Pang, K.; Quan, S. M.; Parkin, G. Tetrahedral nickel nitrosyl complexes with tripodal $[N_3]$ and $[Se_3]$ donor ancillary ligands: structural and computational evidence that a linear nitrosyl is a trivalent ligand. *Dalton Trans.* **2007**, 820−824.
(28) Parkin, G. Impact of the coordination of multiple Lewis acid functions on the electronic structure and v^n configuration of a metal center. *Dalton Trans.* **2022**, *51*, 411−427.
(29) (a) Parkin, G.; Green, M. L. H. Application of the Covalent Bond Classification Method for the Teaching of Inorganic Chemistry. *J. Chem. Educ.* **2014**, *91*, 807−816. (b) Parkin, G. Valence, Oxidation Number, and Formal Charge: Three Related but Fundamentally Different Concepts. *J. Chem. Educ.* **2006**, *83*, 791−799.
(30) Manoharan, P. T.; Gray, H. B. Electronic Structures of Metal Pentacyanonitrosyls. *Inorg. Chem.* **1966**, 823−839.
(31) Hummel, P.; Gray, H. B. Strikingly similar electronic structures of $[Mn(N)(CN)_5]^{3-}$ and $[Mn(NO)(CN)_5]^{3-}$. *Coord. Chem. Rev.* **2007**, *251*, 554−556.
(32) Hummel, P.; Winkler, J. R.; Gray, H. B. Electronic structures of tetragonal nitrido and nitrosyl complexes. *Theor. Chem. Acc.* **2008**, *119*, 35−38.
(33) Wolczanski, P. T. Flipping the Oxidation State Formalism: Charge Distribution in Organometallic Complexes as Reported by Carbon Monoxide. *Organometallics* **2017**, *36*, 622−631.
(34) (a) DiMucci, I. M.; Lukens, J. T.; Chatterjee, S.; Carsch, K. M.; Titus, C. J.; Lee, S. J.; Nordlund, D.; Betley, T. A.; MacMillan, S. N.; Lancaster, K. M. The Myth of d^8 Copper(III). *J. Am. Chem. Soc.* **2019**, *141*, 18505−18520. (b) Walroth, R. C.; Lukens, J. T.; MacMillan, S. N.; Finkelstein, K. D.; Lancaster, K. M. Spectroscopic Evidence for a $3d^{10}$ Ground State Electronic Configuration and Ligand Field Inversion in $[Cu(CF_3)_4]^{1-}$. *J. Am. Chem. Soc.* **2016**, *138*, 1922−1931. (c) Shearer, J.; Vasiliauskas, D.; Lancaster, K. M. Bonding and the role of electrostatics in driving C−C bond formation in high valent organocopper compounds. *Chem. Commun.* **2022**, *59*, 98−101. (d) Carsch, K. M.; DiMucci, I. M.; Iovan, D. A.; Li, A.; Zheng, S. L.; Titus, C. J.; Lee, S. J.; Irwin, K. D.; Nordlund, D.; Lancaster, K. M.; Betley, T. A. Synthesis of a copper-supported triplet nitrene complex pertinent to copper-catalyzed amination. *Science* **2019**, *365*, 1138−1143.
(35) Shreiber, S. T.; DiMucci, I. M.; Khrizanforov, M. N.; Titus, C. J.; Nordlund, D.; Dudkina, Y.; Cramer, R. E.; Budnikova, Y.; Lancaster, K. M.; Vicic, D. A. $[(MeCN)Ni(CF_3)_3]^-$ and $[Ni(CF_3)_4]^{2-}$: Foundations toward the Development of Trifluoromethylations at Unsupported Nickel. *Inorg. Chem.* **2020**, *59*, 9143−9151.
(36) Desnoyer, A. N.; He, W.; Behyan, S.; Chiu, W.; Love, J. A.; Kennepohl, P. The Importance of Ligand-Induced Backdonation in the Stabilization of Square Planar d^{10} Nickel π-Complexes. *Chem. − Eur. J.* **2019**, *25*, 5259−5268.
(37) Mena, M. R.; Kim, J.-H.; So, S.; Ben-Daat, H.; Porter, T. M.; Ghosh, C.; Sharma, A.; Flores, M.; Groy, T. L.; Baik, M.-H.; Trovitch, R. J. Comparing the Electronic Structure of Iron, Cobalt and Nickel Compounds That Feature a Phosphine-Substituted Bis(imino)pyridine Chelate. *Inorg. Chem.* **2022**, *61*, 6438−6450.
(38) Duncan, A. P.; Johnson, A. R.; Nataro, C. Literature-Based Teaching Strategies for Organometallic Courses. *Organometallics* **2017**, *36*, 2703−2705.
(39) Koch, D.; Manzhos, S. The role of solvent charge donation in the stabilization of metal ions in aqueous solution. *MRS Commun.* **2018**, *8*, 1139−1144.
(40) Hayton, T. W.; Legzdins, P.; Brett Sharp, W. Coordination and Organometallic Chemistry of Metal-NO Complexes. *Chem. Rev.* **2002**, *102*, 935−992.
(41) Bohnenberger, J.; Schmitt, M.; Feuerstein, W.; Krummenacher, I.; Butschke, B.; Czajka, J.; Malinowski, P. J.; Breher, F.; Krossing, I. Completing the triad: synthesis and full characterization of homoleptic and heteroleptic carbonyl and nitrosyl complexes of the group VI metals. *Chem. Sci.* **2020**, *11*, 3592−3603.

https://doi.org/10.1021/acs.organomet.3c00197
Organometallics 2023, 42, 2747−2761

(42) Klein, A.; von Mering, Y.; Uthe, A.; Butsch, K.; Schaniel, D.; Mockus, N.; Woike, T. Oxidation States and photoinduced metastable states in $[Fe(CO)_2(NO)_2]$. *Polyhedron* **2010**, *29*, 2553−2559.
(43) Schmitt, M.; Mayländer, M.; Goost, J.; Richert, S.; Krossing, I. Chasing the Mond Cation: Synthesis and Characterization of the Homoleptic Nickel Tetracarbonyl Cation and its Tricarbonyl-Nitrosyl Analogue. *Angew. Chem., Int. Ed.* **2021**, *60*, 14800−14805.
(44) Song, Z.; Wang, X. Ruthenium and osmium carbonyl nitrosyl complexes: Matrix infrared spectra and density functional calculations for $M(CO)_2(NO)_2$ and M(CO)(NO) (M = Ru, Os). *Chem. Phys.* **2012**, *407*, 134−142.
(45) (a) Andrews, L.; Citra, A. Infrared Spectra and Density Functional Theory Calculations on Transition Metal Nitrosyls. Vibrational Frequencies of Unsaturated Transition Metal Nitrosyls. *Chem. Rev.* **2002**, *102*, 885−912. (b) Citra, A.; Andrews, L. Reactions of Laser-Ablated Rhodium and Iridium Atoms with Nitric Oxide in Neon and Argon. Matrix Infrared Spectra and Density Functional Calculations of $Rh(NO)_{1-3}$, $Ir(NO)_{1-3}$, NRhO, $RhNO^+$, and $IrNO^+$. *J. Phys. Chem. A* **2000**, *104*, 11897−11908.
(46) Heberhold, M.; Razavi, A. Tetranitrosyl Chromium $[Cr(NO)_4]$. *Angew. Chem., Int. Ed.* **1972**, *11*, 1092−1094.
(47) Raynar, D. M.; Nazran, A. S.; Drouin, M.; Hackett, P. A. 248-nm Photolysis of Tricarbonylnitrosyl. *J. Phys. Chem.* **1986**, *90*, 2882−2888.
(48) Heins, S. P.; Morris, W. D.; Wolczanski, P. T.; Lobkovsky, E. B.; Cundari, T. R. Nitrene Insertion into CC and CH Bonds of Diamide-diimine Ligated Chromium and Iron Complexes. *Angew. Chem., Int. Ed.* **2015**, *54*, 14407−14411.
(49) Heins, S. P.; Wolczanski, P. T.; Cundari, T. R.; MacMillan, S. N. Redox non-innocence permits catalytic nitrene carbonylation by (dadi)Ti=NAd (Ad = adamantyl). *Chem. Sci.* **2017**, *8*, 3410−3418.
(50) Heins, S. P.; Morris, W. D.; Cundari, T. R.; MacMillan, S. N.; Lobkovsky, E. B.; Livezey, N.; Wolczanski, P. T. Complexes of $[(dadi)Ti(L/X)]^m$ that Reveal Redox Non-innocence, and a Stepwise Carbene Insertion into a Carbon-carbon Bond. *Organometallics* **2018**, *37*, 3488−3501.
(51) Heins, S. P.; Zhang, B.; MacMillan, S. N.; Cundari, T. R.; Wolczanski, P. T. Oxidative Additions to Ti(IV) in $[(dadi)^{4-}]$-Ti^{IV}(THF) Involve Carbon-carbon Bond Formation and Redox Non-innocent Behavior. *Organometallics* **2019**, *38*, 1502−1515.
(52) Hulley, E. B.; Heins, S. P.; Wolczanski, P. T.; Lancaster, K. M.; Lobkovsky, E. B. Azaallyl-derived Ring Formation Via Redox Coupling in First Row Transition Metals. *Polyhedron* **2019**, *159*, 225−233.
(53) (a) Fransceschi, F.; Solari, E.; Scopelliti, R.; Floriani, C. Metal-Mediated Transfer of Electrons between Two Different C−C Single Bonds That Function as Electron-Donor and Electron-Acceptor Units. *Angew. Chem., Int. Ed.* **2000**, *39*, 1685−1687. (b) Crescenzi, R.; Solari, E.; Floriani, C.; Chiesi-Villa, A.; Rizzoli, C. One- and Two-Electron Oxidative Pathways Leading to Cyclopropane-Containing Oxidized Porphyrinogens and C−C-Coupled Porphyrinogens from Alkali Cation- and Transition Metal-*meso*-Octaethylporphyrinogen Complexes. *J. Am. Chem. Soc.* **1999**, *121*, 1695−1706. (c) Gallo, E.; Solari, E.; Re, N.; Floriani, C.; Chiesi-Villa, A.; Rizzoli, C. Carbon-Carbon Bonds Functioning as Electron Shuttles: The Generation of Electron-Rich Manganese(II)-Schiff Base Complexes and Their Redox Chemistry. *J. Am. Chem. Soc.* **1997**, *119*, 5144−5154. (d) Gambarotta, S.; Floriani, C.; Chiesi-Villa, A.; Guastini, C. Carbon-Carbon Bond Formation and Cleavage resulting from a Long-range Metal-promoted Redox Process in the Reactions of Nickel(II) Complexes of N,N'-o-Phenylenebis(salicylideneamine). *J. Chem. Soc., Chem. Commun.* **1982**, 756−758.
(54) Bachmann, J.; Nocera, D. G. Multielectron Redox Chemistry of Iron Porphyrinogens. *J. Am. Chem. Soc.* **2005**, *127*, 4730−4743.
(55) Bhattacharya, D.; Dey, S.; Maji, S.; Pal, K.; Sarkar, S. Direct Incorporation of a Ferric Ion in the Porphyrinogen Core: Tetrakis-(cyclohexyl)iron Porphyrinogen Anion with Different Conformers and Its Reaction with Iodine. *Inorg. Chem.* **2005**, *44*, 7699−7701.
(56) Zavitsas, A. A. The Relation between Bond Lengths and Dissociation Energies of Carbon-Carbon Bonds. *J. Phys. Chem. A* **2003**, *107*, 897−898.
(57) Hulley, E. B.; Wolczanski, P. T.; Lobkovsky, E. B. Carbon-carbon Bond Formation from Azaallyl and Imine Couplings About Metal-metal Bonds. *J. Am. Chem. Soc.* **2011**, *133*, 18058−18061.
(58) Bradley, D. C.; Hursthouse, M. B.; Newing, C. W.; Welch, A. J. Square planar and tetrahedral chromium(II) complexes; crystal structure determinations. *J. Chem. Soc., Chem. Commun.* **1972**, 567−568.
(59) (a) Bürger, H.; Wannagat, U. Silylamido-Derivate von Eisen und Kobalt. *Monatsh. Chem.* **1963**, *94*, 1007−1012. (b) Anderson, R. A.; Faegri, K., Jr.; Green, J. C.; Haaland, A.; Lappert, M. F.; Leungand, W.-P.; Rypdal, K. Synthesis of bis[bis(trimethylsilyl)amido]iron(II). Structure and bonding in $M[N(SiMe_3)_2]_2$ (M = manganese, iron, cobalt): two-coordinate transition-metal amides. *Inorg. Chem.* **1988**, *27*, 1782−1786.
(60) Bryan, A. M.; Long, G. J.; Grandjean, F.; Power, P. P. Synthesis, Spectroscopic Characterization, and Determination of the Solution Association Energy of the Dimer $[Co\{N(SiMe_3)_2\}_2]_2$: Magnetic Studies of Low-Coordinate Co(II) Silylamides $[Co\{N(SiMe_3)_2\}_2L]$ (L = PMe_3, Pyridine, and THF) and Related Species That Reveal Evidence of Very Large Zero-Field Splittings. *Inorg. Chem.* **2013**, *52*, 12152−12160.
(61) (a) Evans, D. F. The Determination of the Paramagnetic Susceptibility of Substances in Solution by Nuclear Magnetic Resonance. *J. Chem. Soc.* **1959**, 2003−2005. (b) Schubert, E. M. Utilizing the Evans Method with a Superconducting NMR Spectrometer in the Undergraduate Laboratory. *J. Chem. Ed.* **1992**, *69*, 62.
(62) Figgis, B. N.; Hitchman, M. A. *Ligand Field Theory and Its Applications*; Wiley-VCH: New York, 2000.
(63) Ona, O. B.; Alcoba, D. R.; Massaccesi, G. E.; Torre, A.; Lain, L.; Melo, J. I.; Oliva-Enrich, J. M.; Peralta, J. E. Magnetic Properties of Co(II) Complexes with Polyhedral Carborane Ligands. *Inorg. Chem.* **2019**, *58*, 2550−2557.
(64) Hoffmann, S. K.; Goslar, J.; Lijewski, S. Electron Paramagnetic Resonance and Electron Spin Echo Studies of Co2+ Coordination by Nicotinamide Adenine Dinucleotide (NAD+) in Water Solution. *Appl. Magn. Reson.* **2013**, *44*, 817−826.
(65) van Leest, N. P.; Stroek, W.; Siegler, M. A.; van der Vlugt, J. I.; de Bruin, B. Ligand-Mediated Spin-State Changes in a Cobalt-Dipyrrin-Bisphenol Complex. *Inorg. Chem.* **2020**, *59*, 12903−12912.
(66) Kochem, A.; Chiang, L.; Baptiste, B.; Philouze, C.; Leconte, N.; Jarjayes, O.; Storr, T.; Thomas, F. Ligand-Centered Redox Activity in Cobalt(II) and Nickel(II) Bis(Phenolate)−Dipyrrin Complexes. *Chem. − Eur. J.* **2012**, *18*, 14590−14593.
(67) Okuniewski, A.; Rosiak, D.; Chojnacki, J.; Becker, B. Coordination polymers and molecular structures among complexes of mercury(II) halides with selected 1-benzoylthioureas. *Polyhedron* **2015**, *90*, 47−57.
(68) Yang, L.; Powell, D. R.; Houser, R. P. Structural variation in copper(I) complexes with pyridylmethylamide ligands: structural analysis with a new four-coordinate geometry index, τ_4. *Dalton Trans.* **2007**, 955−964.
(69) Allen, F. H.; Kennard, O.; Watson, D. G.; Brammer, L.; Orpen, A. G.; Taylor, R. Tables of Bond Lengths determined by X-ray and Neutron Diffraction. Part 1. Bond Lengths in Organic Compounds. *J. Chem. Soc., Perkin Trans. 2* **1987**, S1−S19.
(70) Pokhriyal, D.; Heins, S. P.; Sifri, R. J.; Genetekos, D. T.; Coleman, R. E.; Wolczanski, P. T.; Fors, B. P.; Cundari, T. R.; Lancaster, K. M.; MacMillan, S. N. Reversible C−C Bond Formation, Halide Abstraction, and Electromers in Complexes of Iron Containing Redox Noninnocent Pyridine-imine Ligands. *Inorg. Chem.* **2021**, *60*, 18662−18673.
(71) (a) Walter, M. R.; Dzul, S. P.; Rodrigues, A. V.; Stemmler, T. L.; Telser, J.; Conradie, J.; Ghosh, A.; Harrop, T. C. Synthesis of Co^{II}-NO^- Complexes and Their Reactivity as a Source of Nitroxyl. *J. Am. Chem. Soc.* **2016**, *138*, 12459−12471. (b) Abucayon, E. G.; Khade, R. L.; Powell, D. R.; Zhang, Y.; Richter-Addo, G. B. Not Limited to Iron: A Cobalt Heme-NO Model Facilitates N-N Coupling with External NO

https://doi.org/10.1021/acs.organomet.3c00197
Organometallics 2023, 42, 2747−2761

in the Presence of a Lewis Acid to Generate N_2O. *Angew. Chem., Int. Ed.* **2019**, *58*, 18598−18603.
(72) Addison, A. W.; Rao, N. T.; Reedijk, J.; van Rijn, J.; Verschoor, G. C. Synthesis, structure, and spectroscopic properties of copper(II) compounds containing nitrogen−sulfur donor ligands; the crystal and molecular structure of aqua[1,7-bis(N-methylbenzimidazol-2′-yl)-2,6-dithiaheptane]copper(II) perchlorate. *J. Chem. Soc., Dalton Trans.* **1984**, 1349−1356.
(73) Hoffmann, R.; Alvarez, S.; Mealli, C.; Falceto, A.; Cahill, T. J., III; Zeng, T.; Manca, G. From Widely Accepted Concepts in Coordination Chemistry to Inverted Ligand Fields. *Chem. Rev.* **2016**, *116*, 8173−8192.

https://doi.org/10.1021/acs.organomet.3c00197
Organometallics 2023, 42, 2747−2761